4. Seasonal Variation in Multi-Radar Coverage for WSR-88D Precipitation Estimation in a Mountainous Region

4.1 Introduction

The WSR-88D Precipitation Processing System (PPS) computes estimates of rainfall out to a radius of 230 km from the radar (Fulton et al. 1998) . In computing the rainfall estimates the PPS also attempts to minimize the impact of terrain induced beam blockages by using the lowest unobstructed tilt which, according to beam geometry and digital elevation model (DEM) data, should clear the terrain by at least 500 ft (O'Bannon, 1997).

Klazura et al (1999) and others have shown that while the computational range of the PPS is 230 km, the true range for valid rainfall estimates is generally less than 230 km due to severe range degradation associated with beam overshoot and partial beam filling. It has also been shown that the problem with range degradation in the precipitation estimates is more severe in stratiform rainfall situations than in convective events. The observation that range effects are more severe in stratiform situations is due to the fact that stratiform precipitation tends to be more shallow than convective precipitation which means that even the lowest tilt is likely to overshoot the precipitation at long range.

Smith et al. (1996) show that tendency for the radar to estimate less precipitation at long ranges from the radar can easily be observed in long term accumulations of a year or more. This range degradation problem can be observed in total accumulation, mean hourly rain rate, and in the probability of detection of rainfall as a function of range. Here we illustrate how these long term accumulations and gridded climatologies of the frequency of rainfall in hourly precipitation products can be used to create a map showing which grid points are well or poorly covered by a given radar for rainfall estimation in a mountainous region.

4.2 Computation of Radar-Derived Precipitation Climatology

The Digital Precipitation Array (DPA) product contains the radar-derived hourly precipitation accumulation in a 131 x 131 array of grid boxes which make up a portion of the national Hydrologic Rainfall Analysis Project (HRAP) grid which has a resolution of approximately 4 km. The National Weather Service Office of Hydrology has been archiving DPA products valid at the top of each hour from all WSR-88Ds as received operationally by River Forecast Centers through AFOS and AWIPS communications since 1996.

Radar-Derived Precipiation Climatologies were computed from the archive of DPA products for 14 radar sites which provide coverage of the North West River Forecast Center (NWRFC) area of responsibility. These radars are located in Washington, Oregon, Northern California, Idaho, Nevada, Montana, Wyoming and Utah and are affected problems common to mountainous regions such as beam blockage, high elevation location of radar site, orographic enhancement of the precipitation, and a large percentage of the precipitation which falls as snow.

To study the variability of coverage as a function of season, the data was sorted into a warm (April through September) and cool season (October through March). Next, the total rainfall, mean hourly rainfall, and the frequency of rainfall at each grid point for the appropriate

seasonal period 1996 through 1999 was computed. The total rainfall was computed by summing up hourly rainfall totals at each grid point excluding missing data. The mean rainfall was computed by dividing the total rainfall by the number of hours in the seasonal period of record excluding missing data. The frequency of precipitation at each grid point was computed by counting the number of hours in which rainfall was observed at a grid point and dividing by the total number of hours DPA products were available.

The frequency of precipitation for both cool and warm season is shown in figures (1a - 28a) for all 14 radar sites used by NWRFC. These figures show that the probability of detecting precipitation drops significantly at long ranges from the radar. The range effect is much more severe in the cool season. There are also several radar sites that appear to be effected by ground clutter caused by areas where the beam too close to the mountains. These areas show up as small regions where the frequency of rainfall is significantly higher than the surrounding grid points.

The effect of beam blockage is apparent in most of the climatologies shown in figures 1-28. Beam blockage can generally be observed as a wedge of lower frequencies extending radially outward. Even when the PPS hybrid scan uses a high tilt to "see" over a blockage, the resulting climatology is likely to show a decrease in the frequency of rainfall at a closer range due to the fact that higher tilts are likely to overshoot the precipitation at a much closer range than a lower tilt. Other blockages caused by trees, buildings and unresolved terrain features in the DEM data which are not accounted for in the PPS hybrid scan can easily be observed in the radar climatologies.

A map showing which grid points are well covered by a given radar can be created by placing a "low" threshold on the frequency climatology below which the radar should not be trusted. Any grid points in which the frequency of precipitation is above the threshold can be considered well covered by the radar. A second "high" threshold can be placed on the radar climatologies to identify areas that are frequently contaminated with ground clutter from mountains. In this case, the grid boxes with frequencies above the "high" threshold are eliminated from the radar coverage map.

The program objectively selects a threshold value as a default which is half of the median frequency observed for all grid points in the field. However, in practice, any objective method for defining the low threshold does not always work well due to nonuniformity of the real precipitation climatology. Furthermore, the extremely variable nature of AP makes an objective selection of an upper threshold even more difficult. Therefore, the program also allows the user to subjectively select high and low thresholds. Fortunately, one or two iterations of manual threshold selection usually yields a satisfactory radar coverage map. Radar coverage maps for both warm and cool season are shown in figures 1b - 28b.

4.3 Multi-Radar Coverage in a Mountainous Region

Warm season and cool season multi-radar coverage maps based on the individual radar coverage maps were created for the entire NWRFC area of forecast responsiblity (figures 29 and 30). Where more than one radar covers a particular grid box, the radar which provides data at the lowest height above sea level was used in the mosaic. Otherwise, a grid point is shown as being covered by a unique radar only if the radar coverage map based on the four year climatology indicates good coverage for that grid point.

The height (above sea level) associated with each pixel in the radar mosaic is shown in figures 31 and 32. Note that in areas where one radar did not have coverage at a low elevation due to a blockage close to the radar site, data from a neighboring radar was used to fill in the missing areas where ever possible. This resulted in the height of coverage being much higher in the blocked areas than it would have been if the closer radar was not blocked.

The main point brought out in figures 29 - 32 is that there are significant gaps in radar coverage for precipitation estimation in the NWRFC area of forecast responsibility. The problem is much worse in the cool season when the climatology is dominated by stratiform events and significantly affected by snow. Figure 30 indicates that radar covers less than half of the NWRFC area of forecast responsibility for precipitation estimation in the cool season. However, even with the significant gaps in coverage, this is an improvement over creating a simple mosaic under the assumption that the radar is capable of producing reliable estimates of precipitation our to a radius of 230 km.

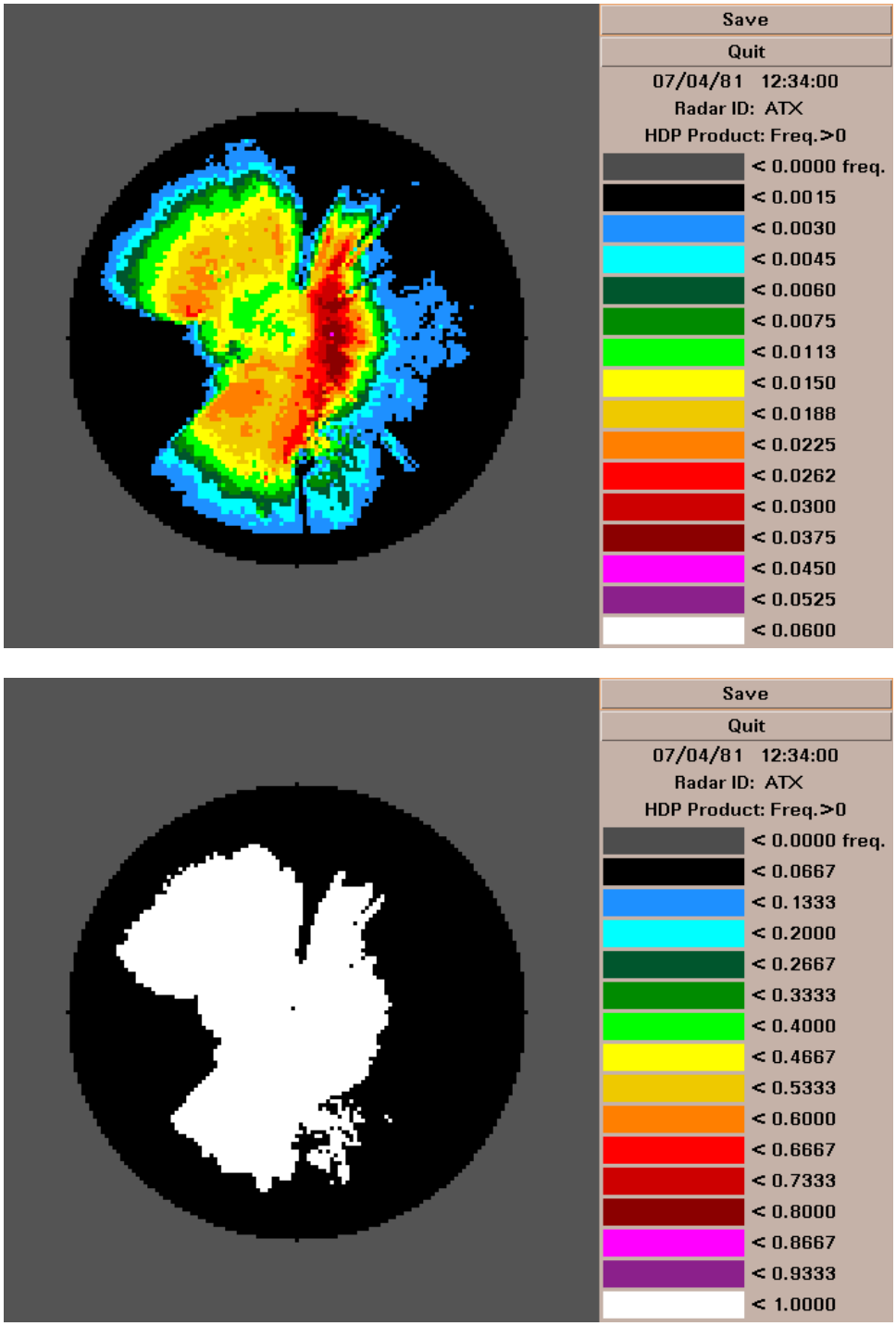

Figure 1. Seattle, Washington (ATX) warm season climatology a) Frequency of Rainfall b) Radar coverage map (white = good coverage)

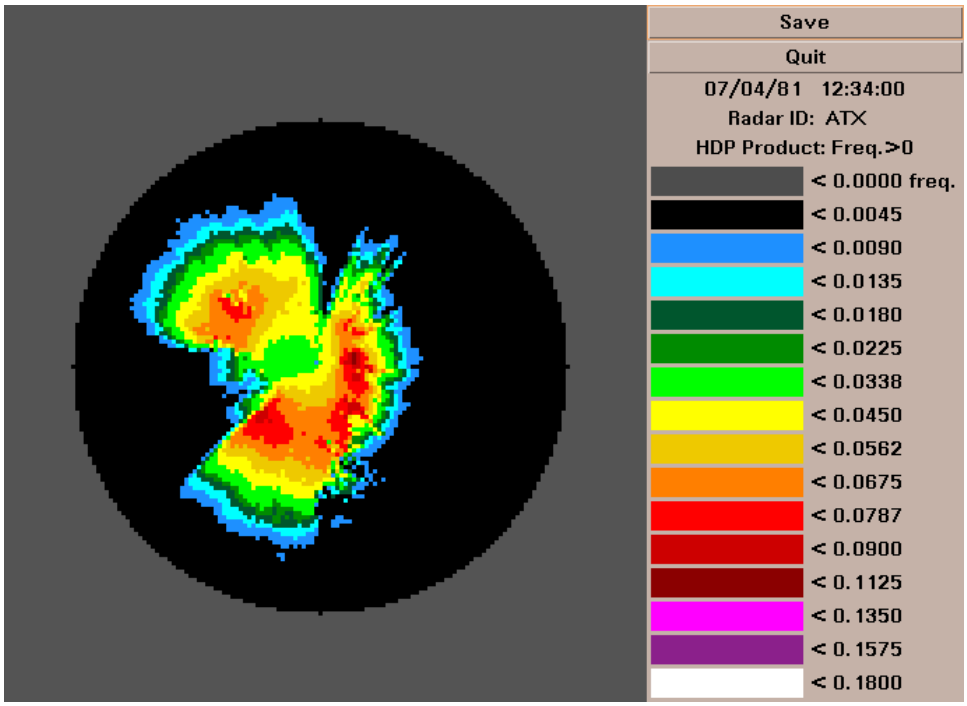

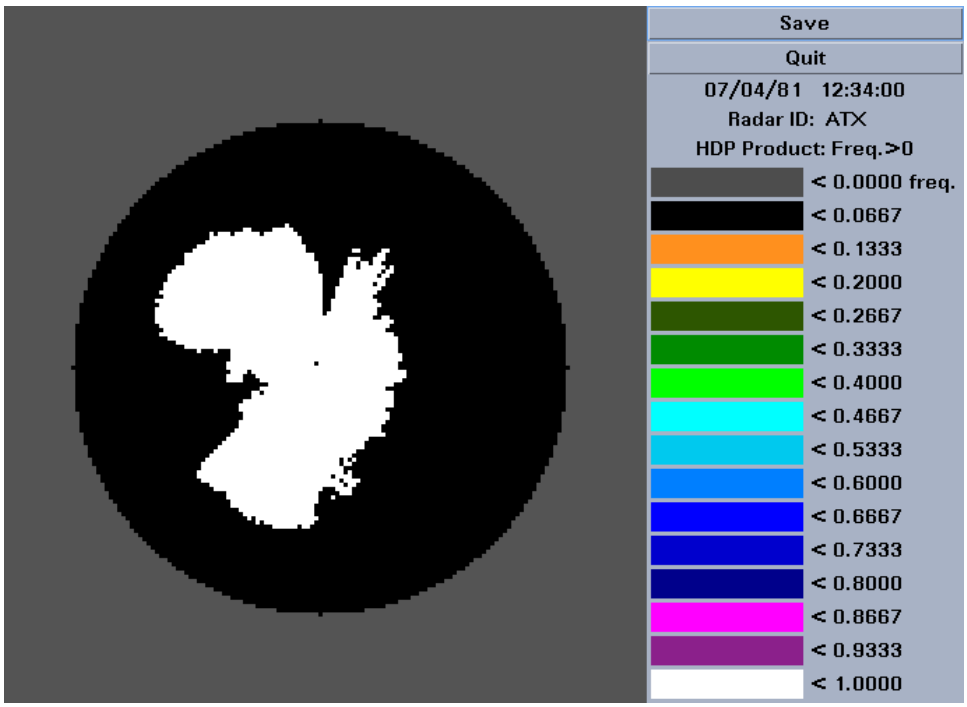

Figure 2. Seattle, Washington (ATX) cool season climatology a) Frequency of Rainfall b) Radar coverage map (white = good coverage)

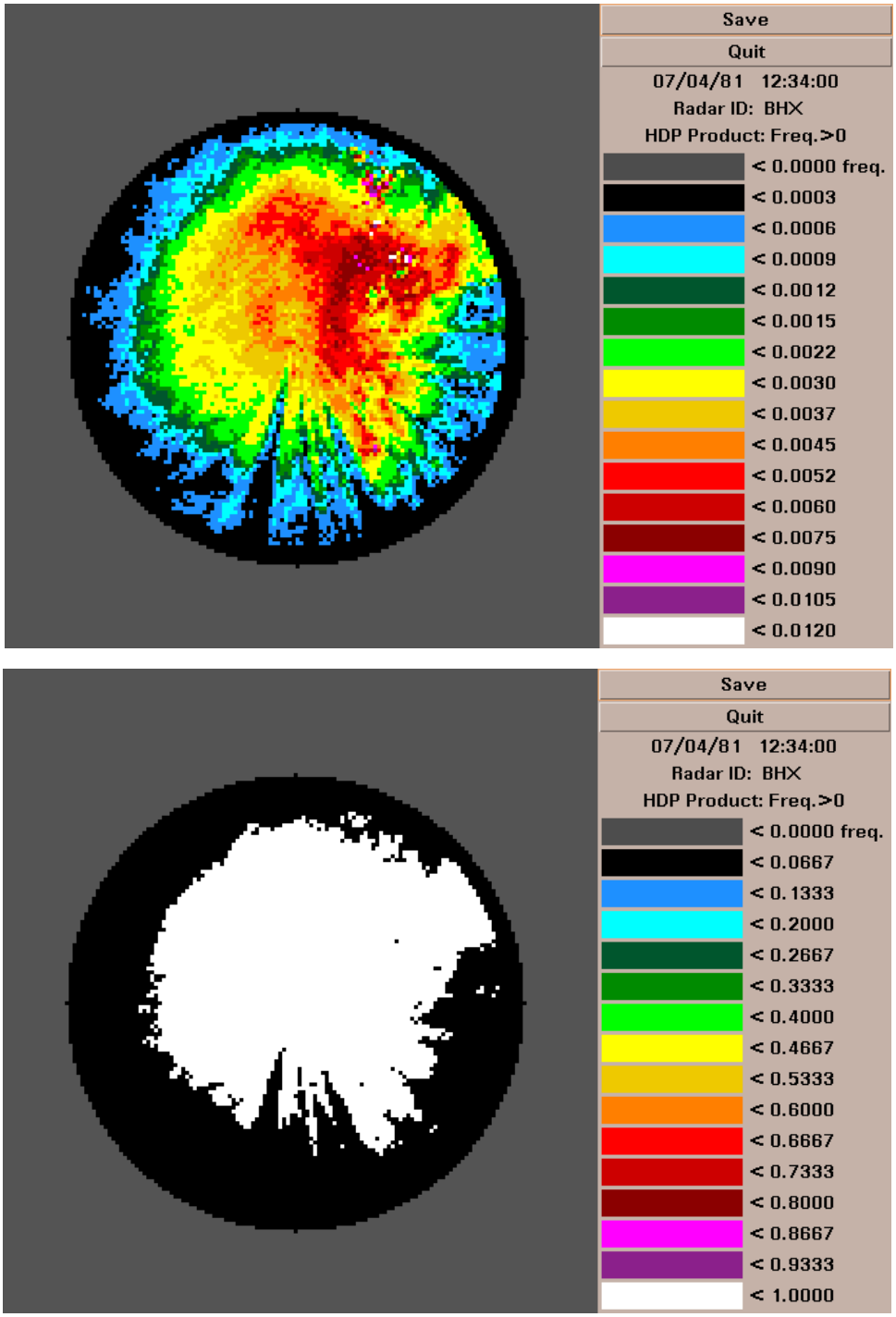

Figure 3. Eureka, CA (BHX) warm season climatology a) Frequency of Rainfall b) Radar coverage map (white = good coverage)

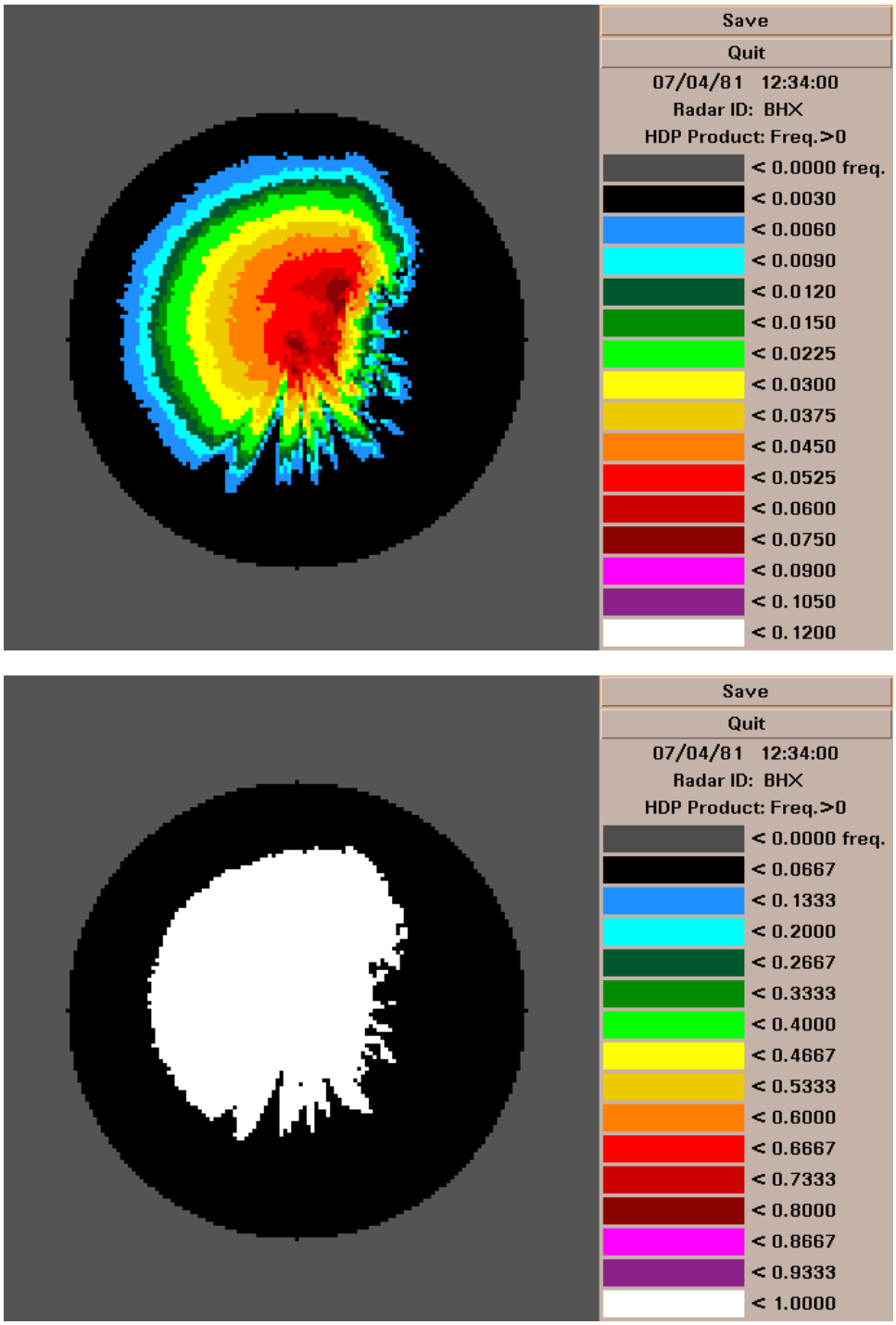

Figure 4. Eureka, CA cool season climatology a) Frequency of Rainfall b) Radar coverage map (white = good coverage)

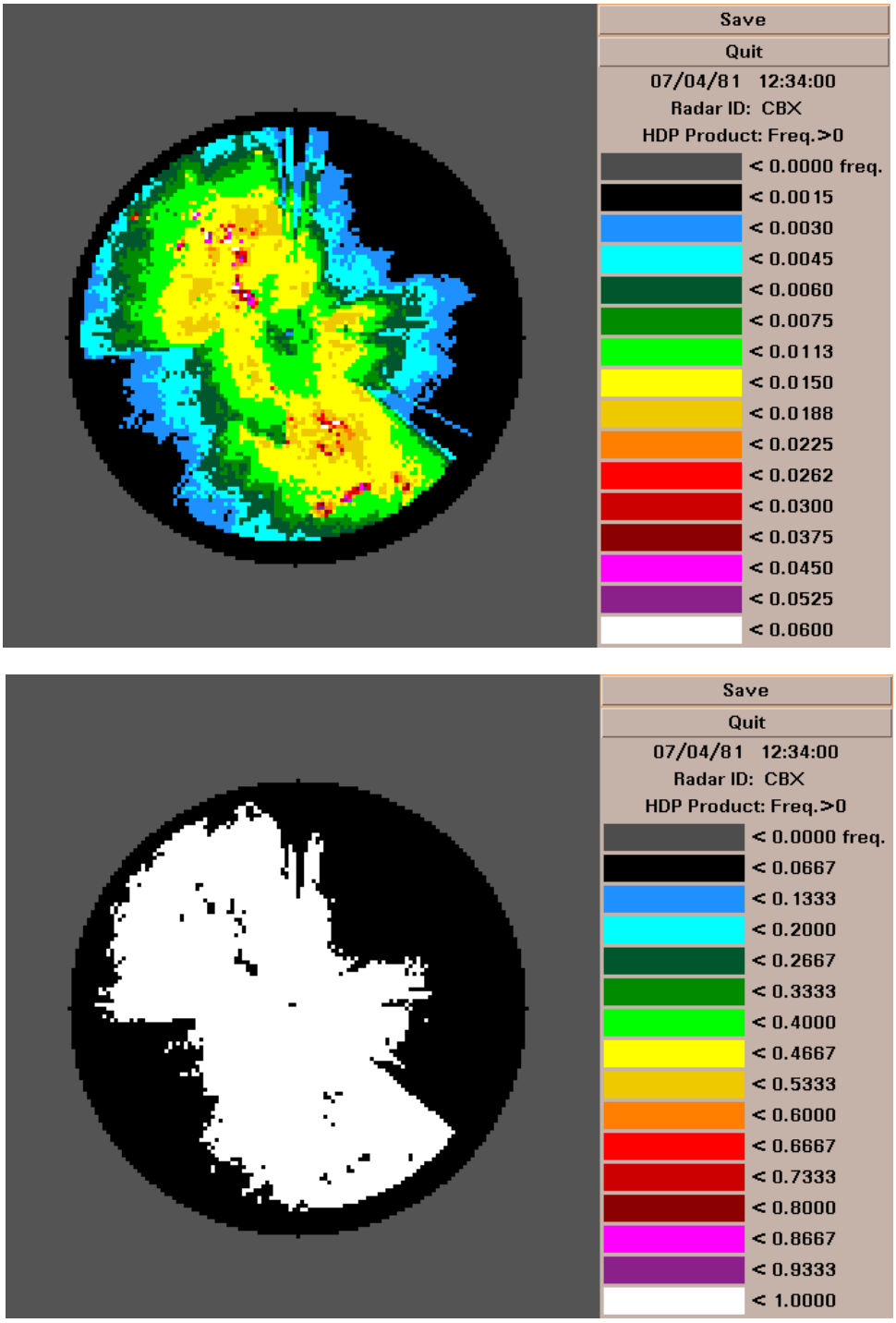

Figure 5. Boise, ID warm season climatology a) Frequency of Rainfall b) Radar coverage map (white = good coverage)

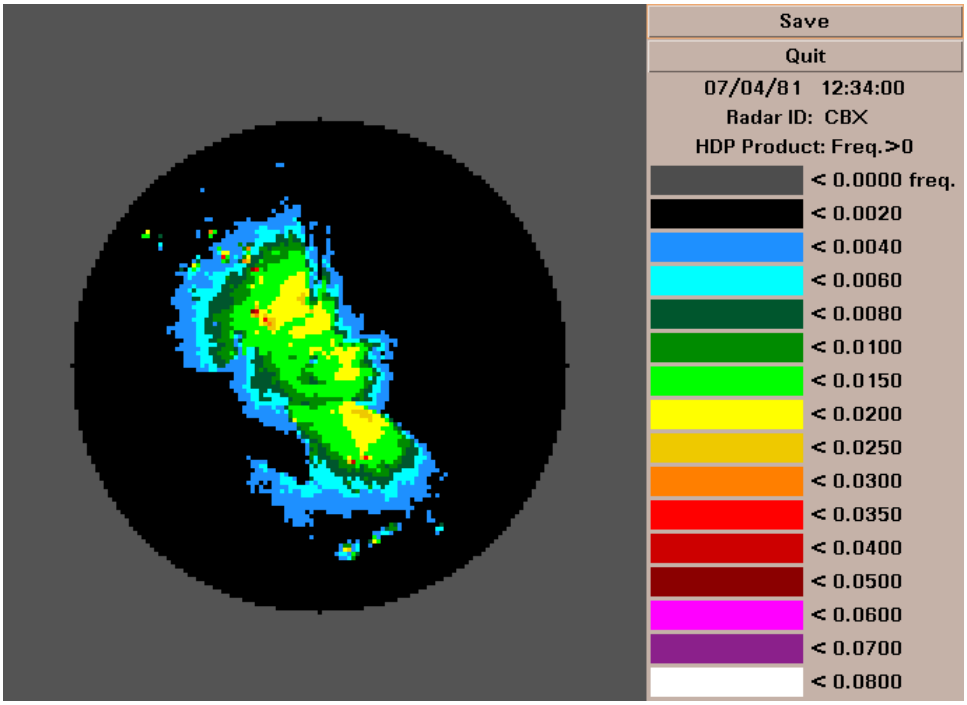

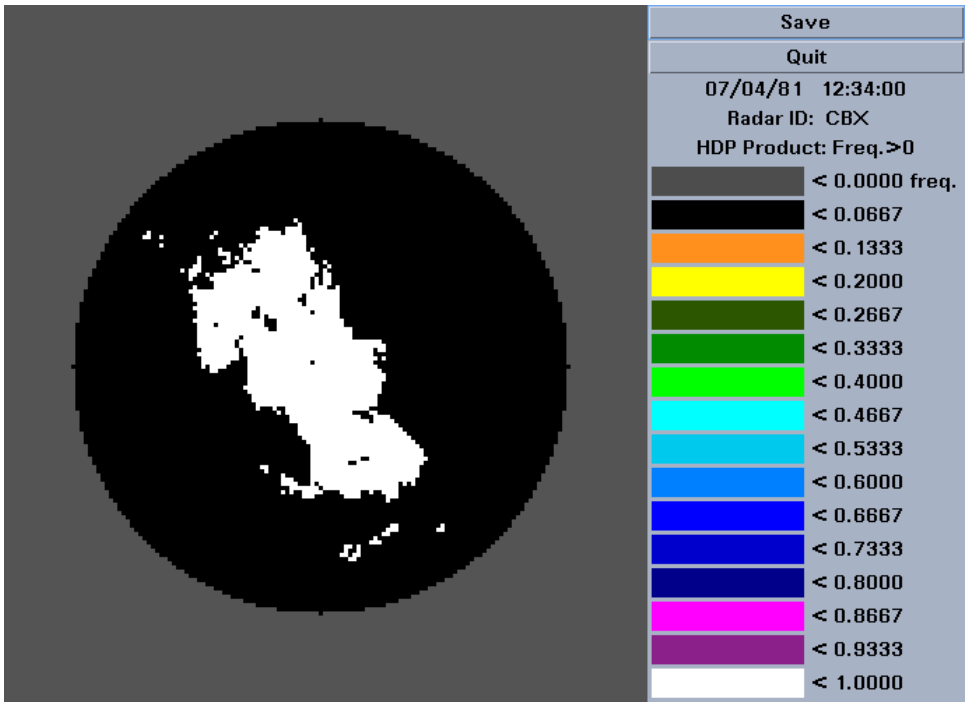

Figure 6. Boise, ID cool season a) Frequency of Rainfall b) Radar coverage map (white = good coverage)

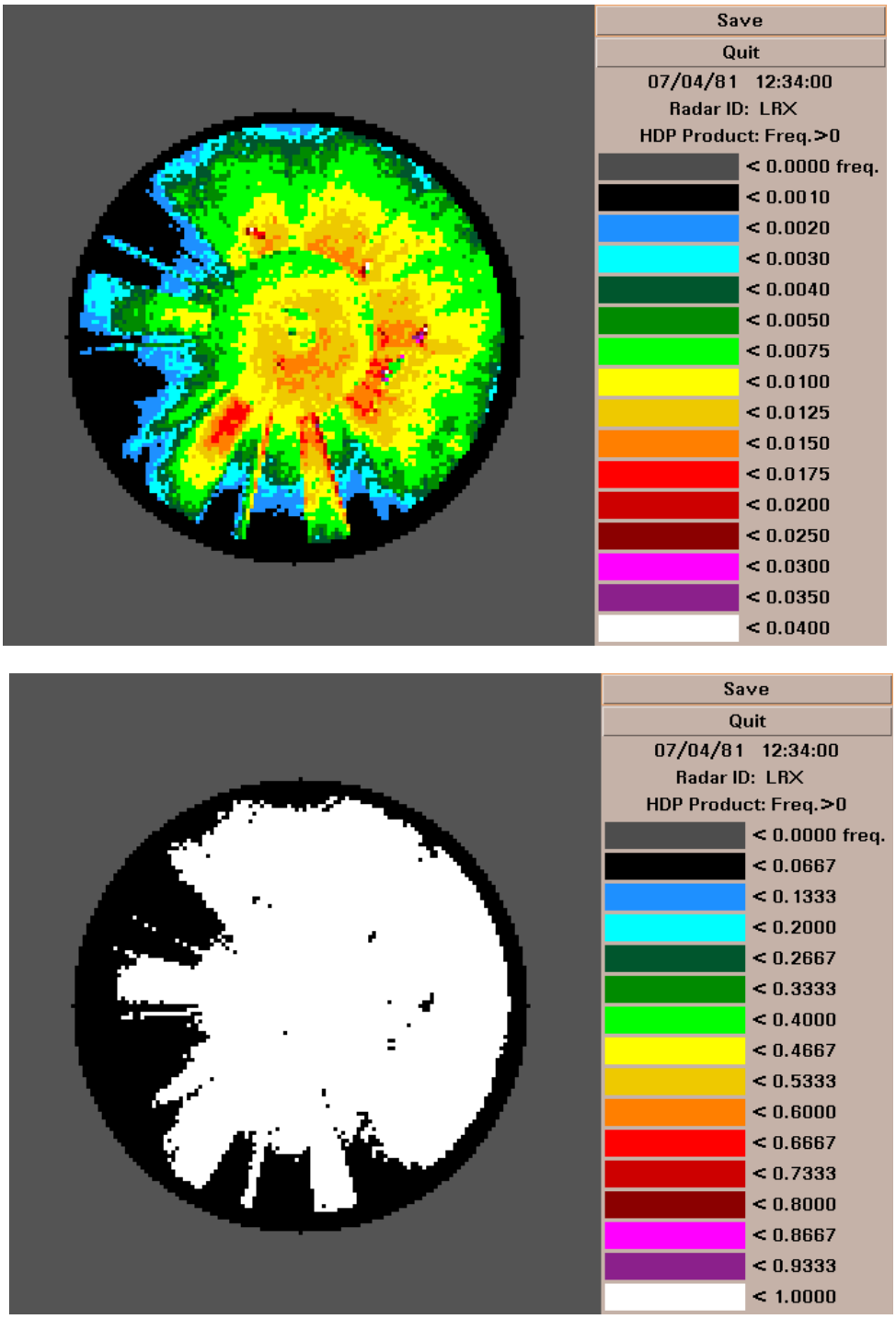

Figure 7. Elko, NV warm season climatology a) Frequency of Rainfall b) Radar coverage map (white = good coverage)

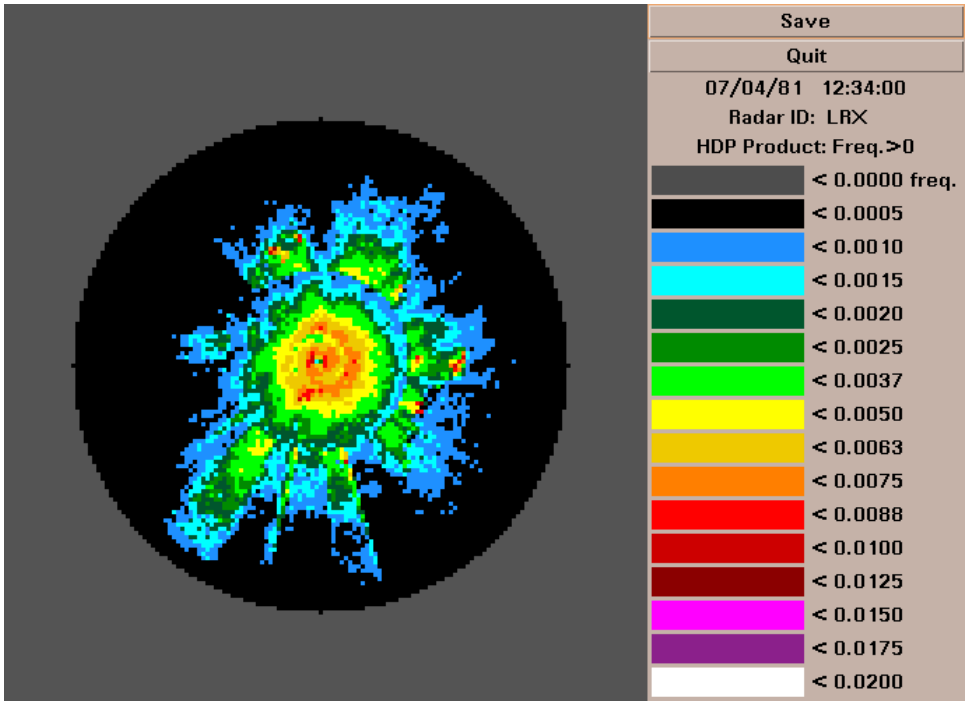

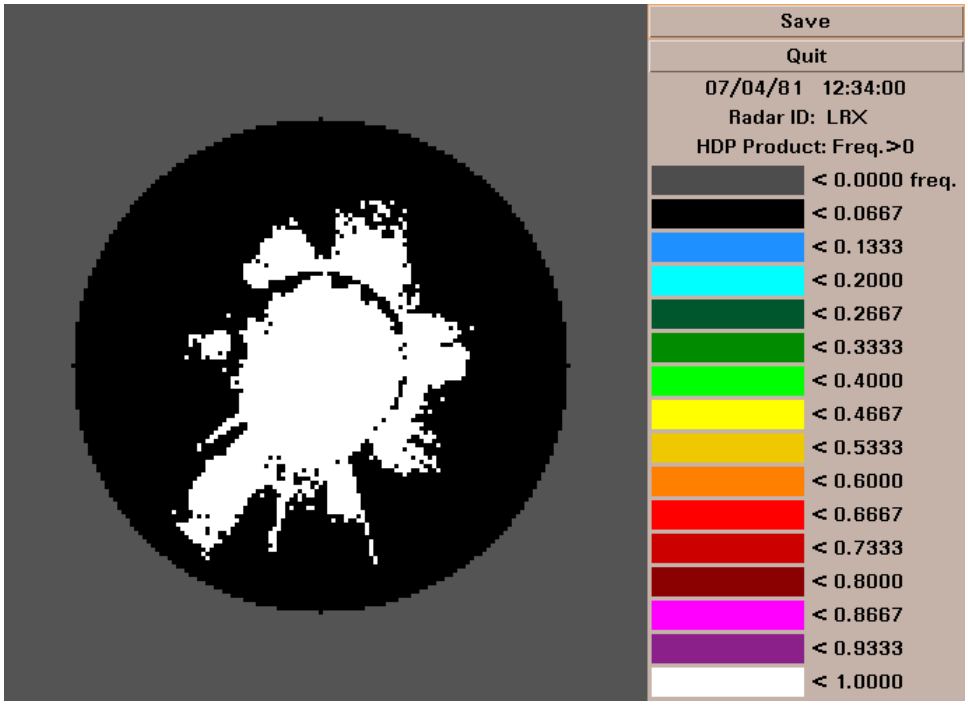

Figure 8. Elko, NV cool season climatology a) Frequency of Rainfall b) Radar coverage map (white = good coverage)

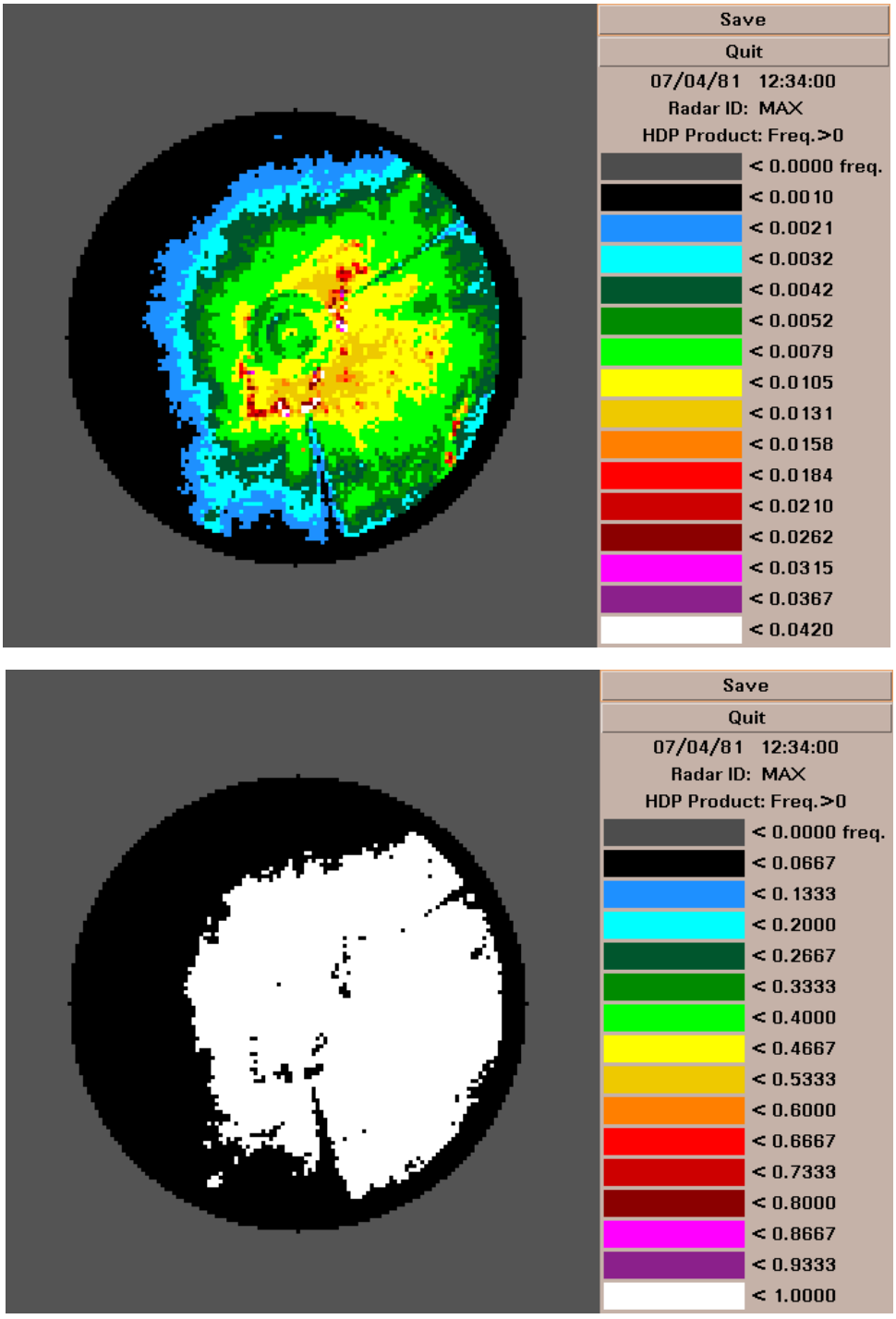

Figure 9. Medford, OR warm season climatology a) Frequency of Rainfall b) Radar coverage map (white = good coverage)

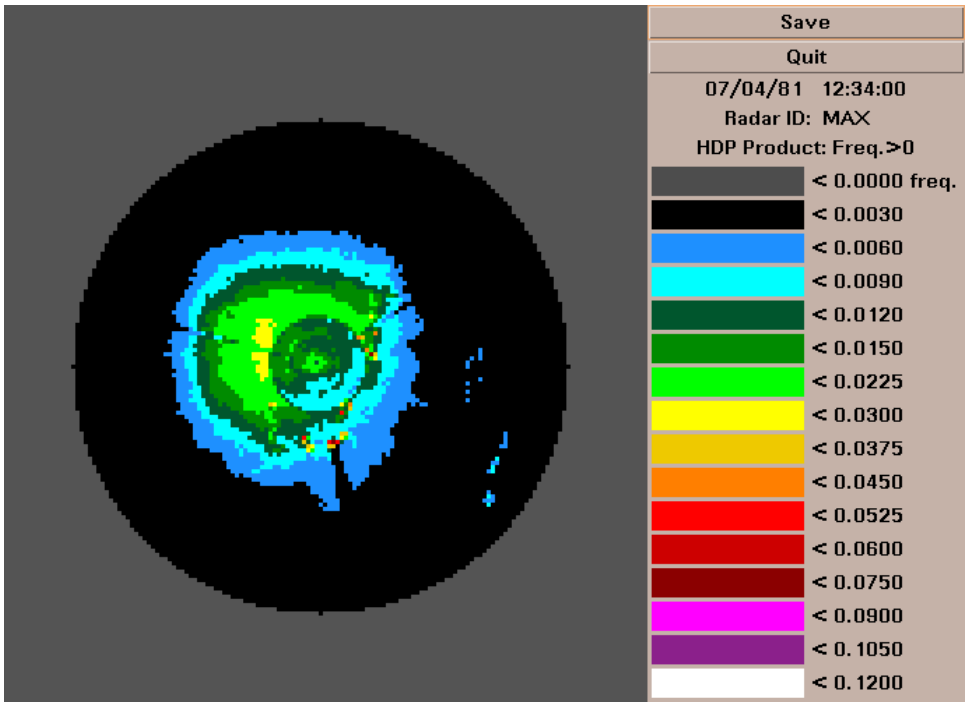

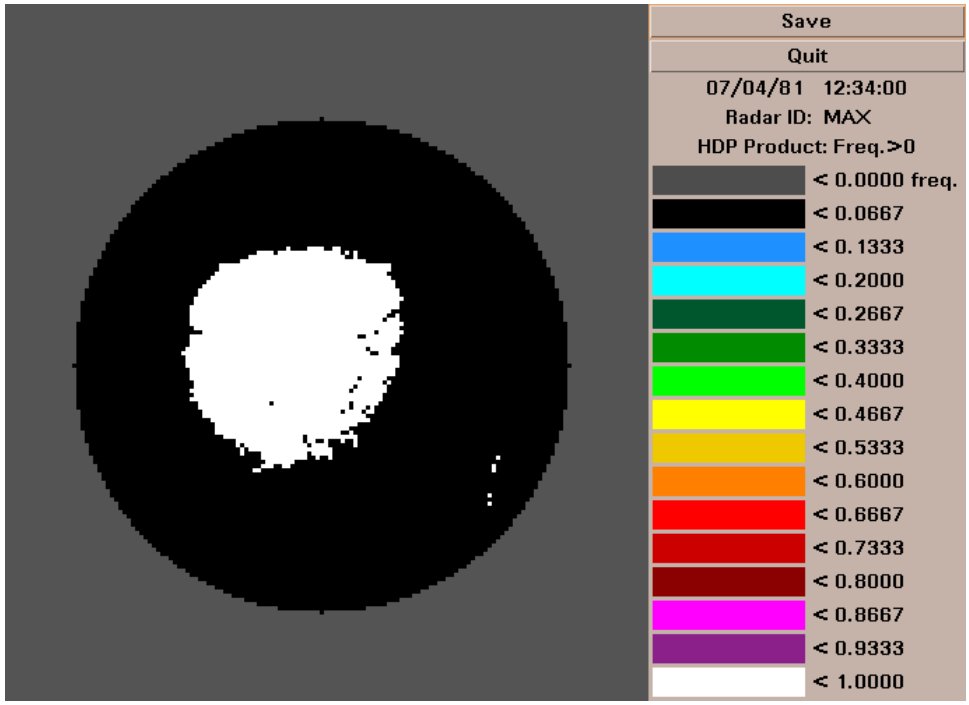

Figure 10. Medford, OR cool season climatology a) Frequency of Rainfall b) Radar coverage map (white = good coverage)

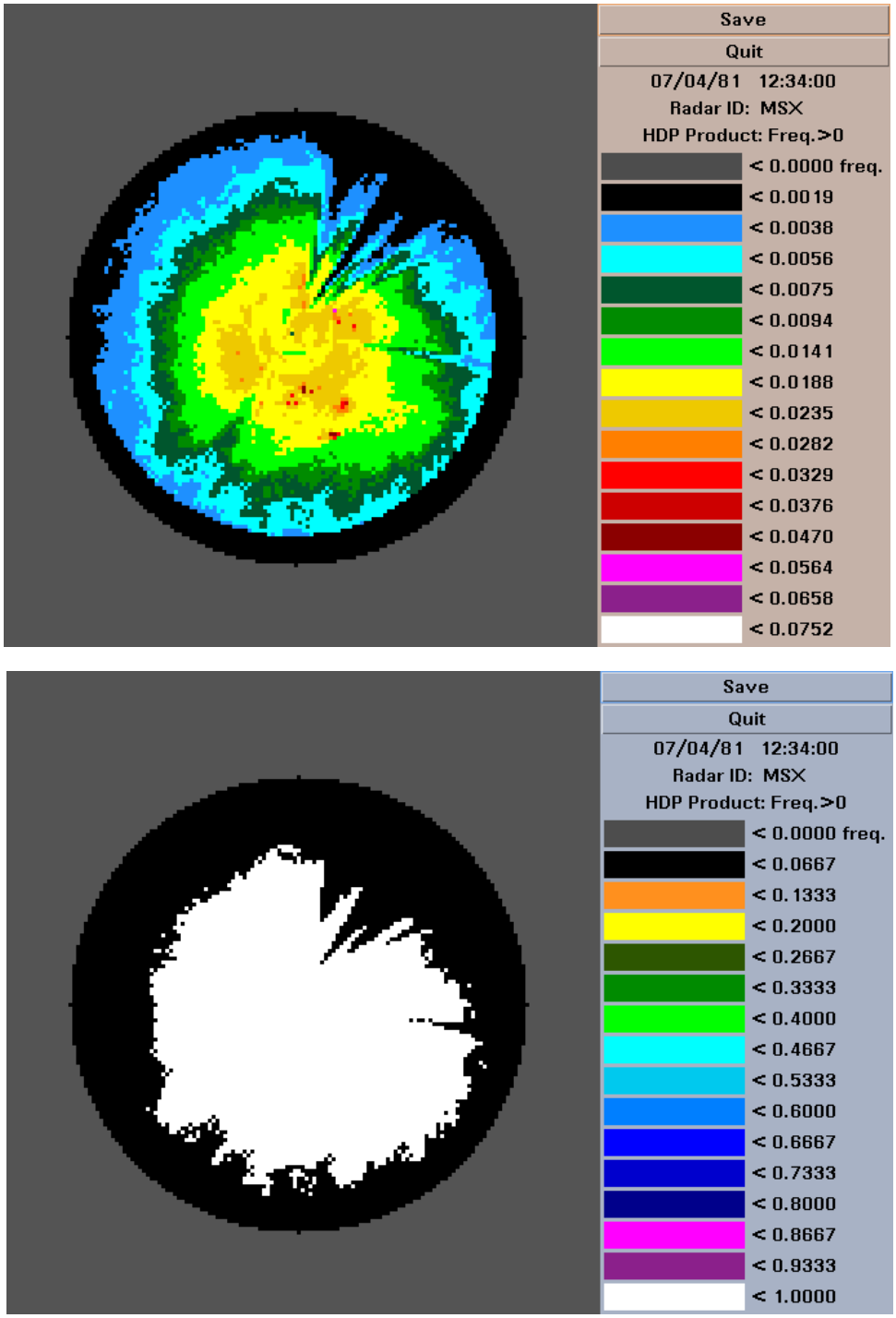

Figure 11. Missoula, MT warm season climatology a) Frequency of Rainfall b) Radar coverage map (white = good coverage)

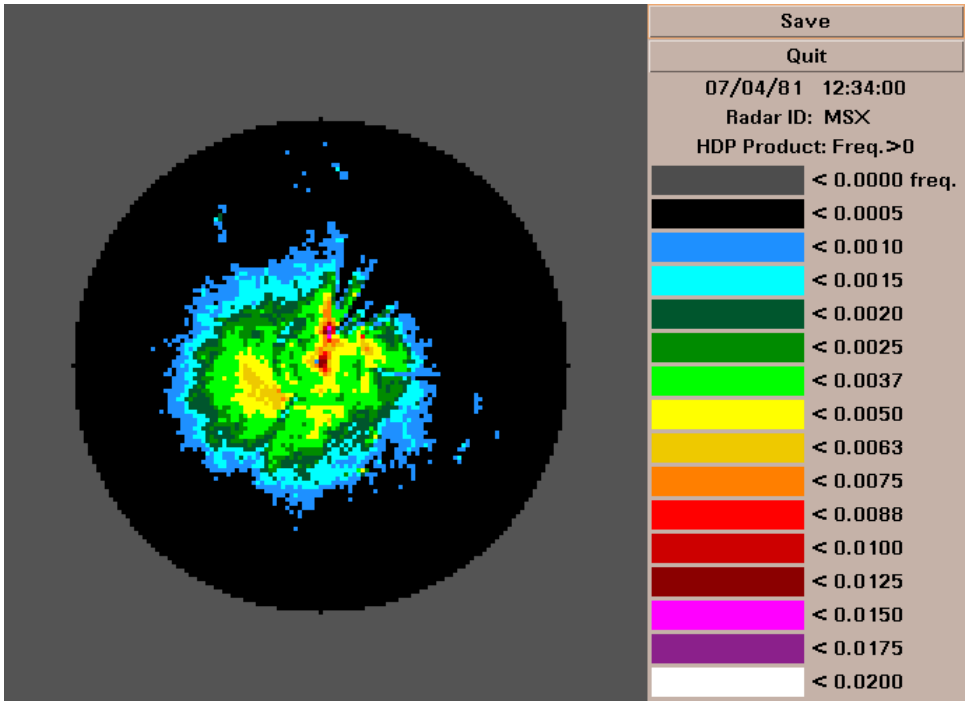

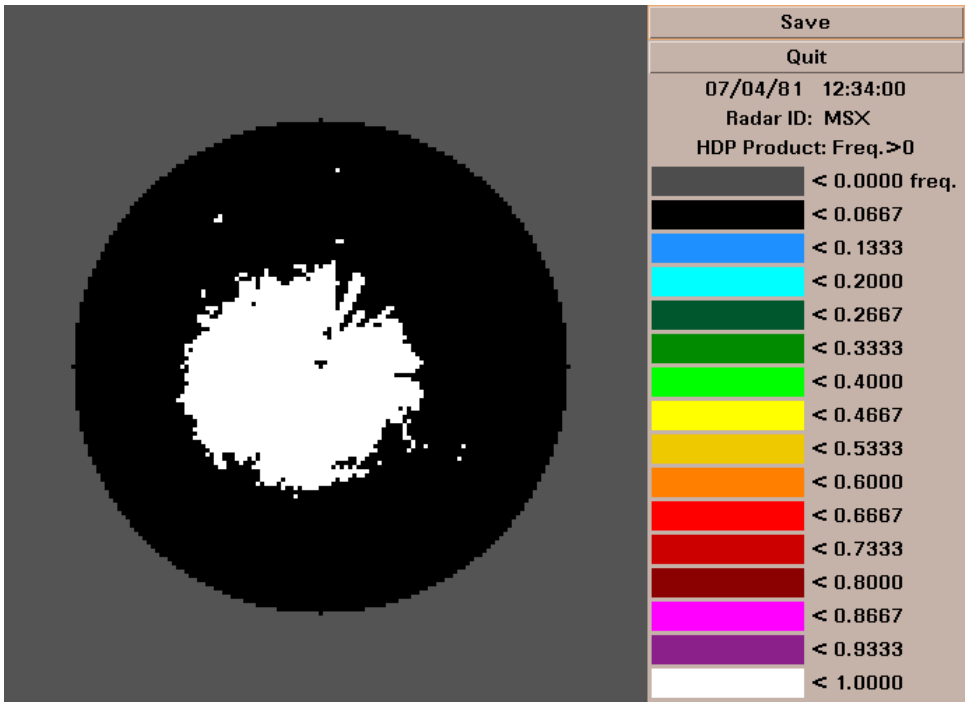

Figure 12. Missoula, MT cool season climatology a) Frequency of Rainfall b) Radar coverage map (white = good coverage)

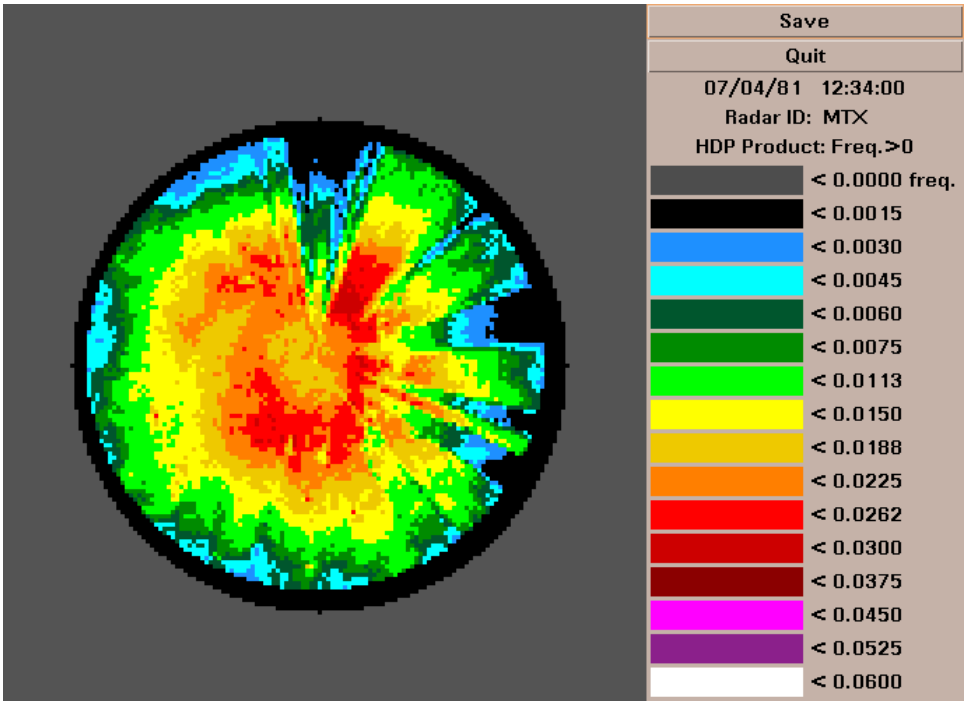

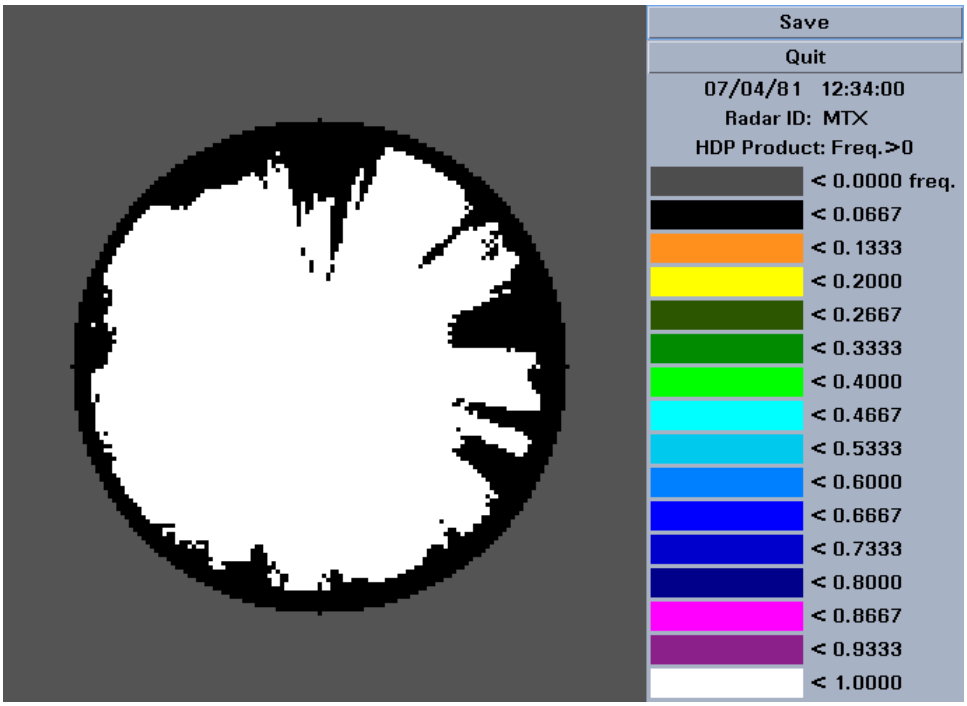

Figure 13. Salt Lake City, UT warm season climatology a) Frequency of Rainfall b) Radar coverage map (white = good coverage)

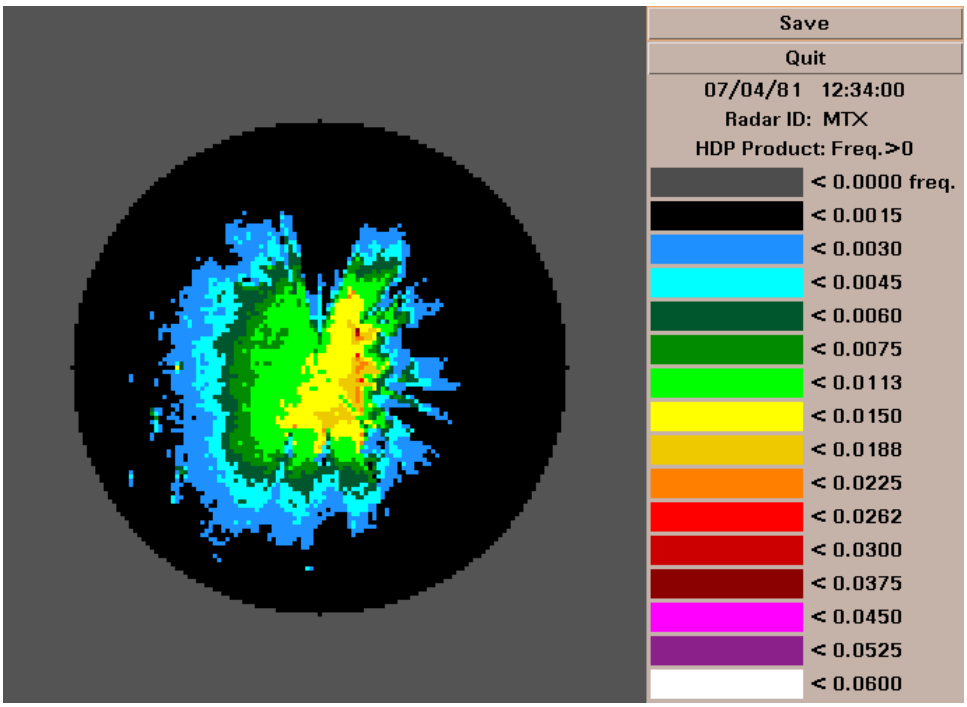

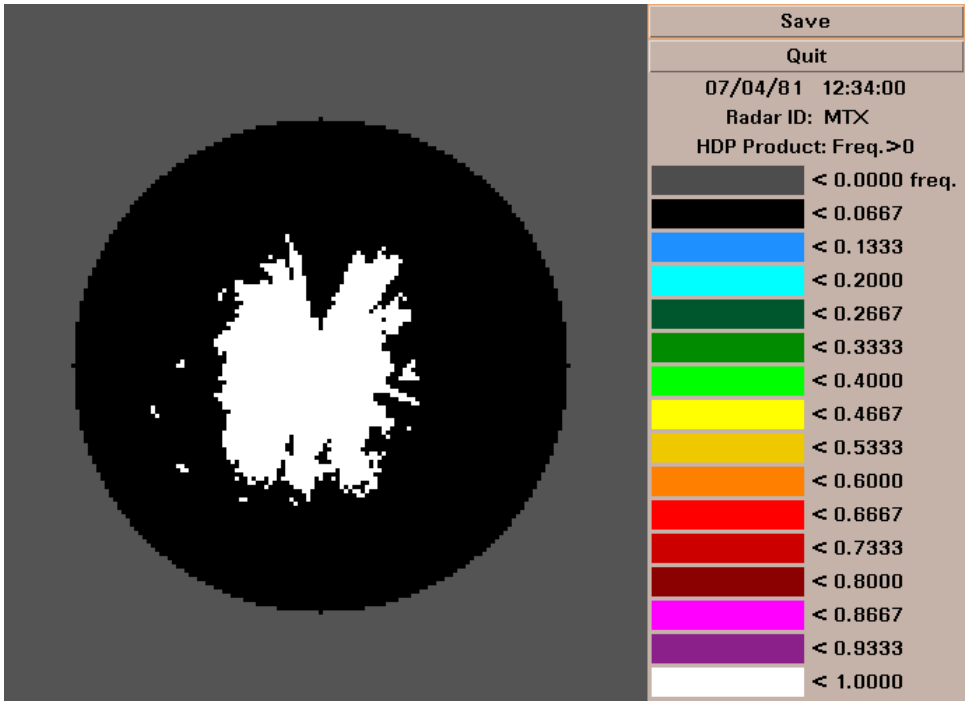

Figure 14. Salt lake City, UT cool season climatology a) Frequency of Rainfall b) Radar coverage map (white = good coverage)

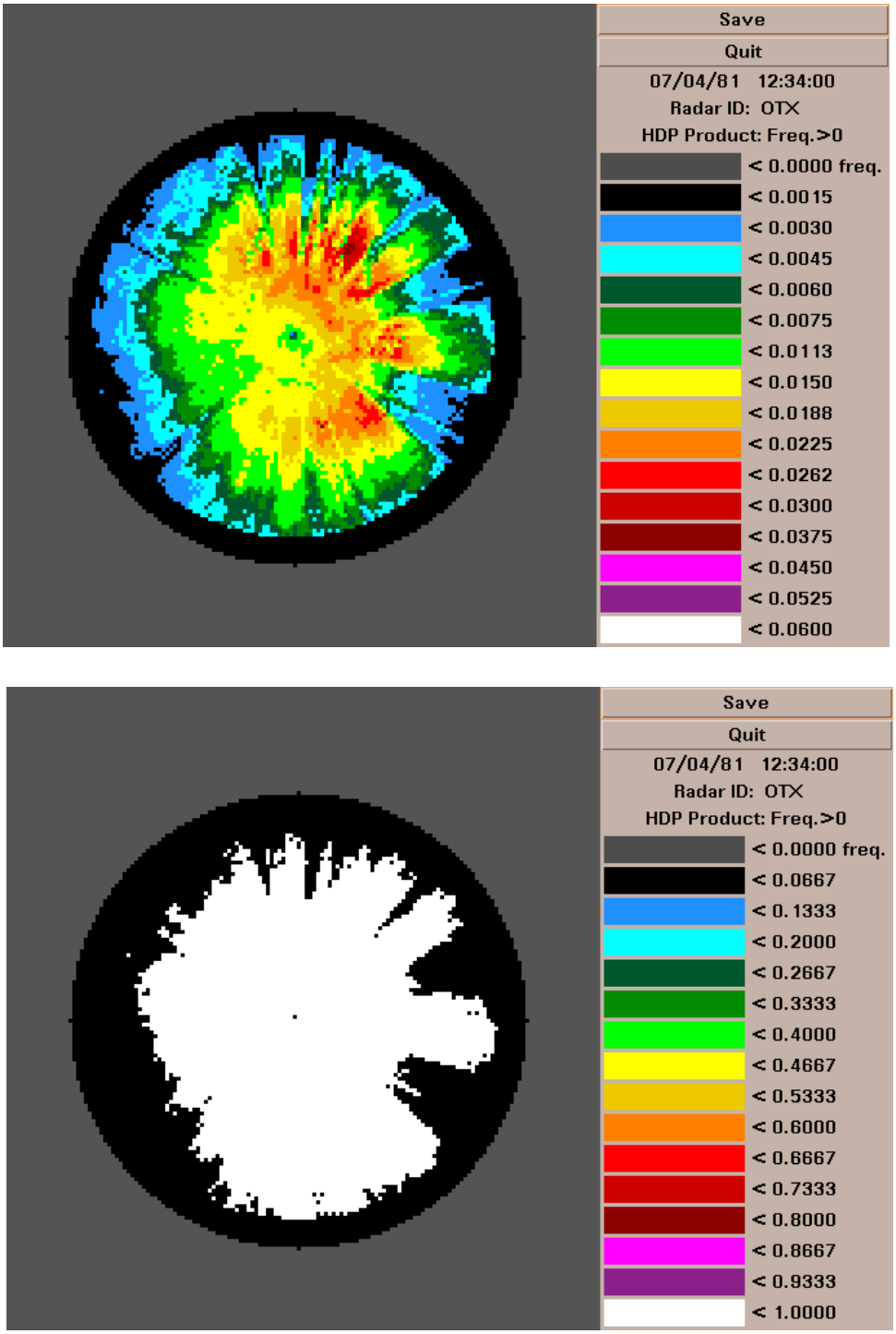

Figure 15. Spokane, WA warm season climatology a) Frequency of Rainfall b) Radar coverage map (white = good coverage)

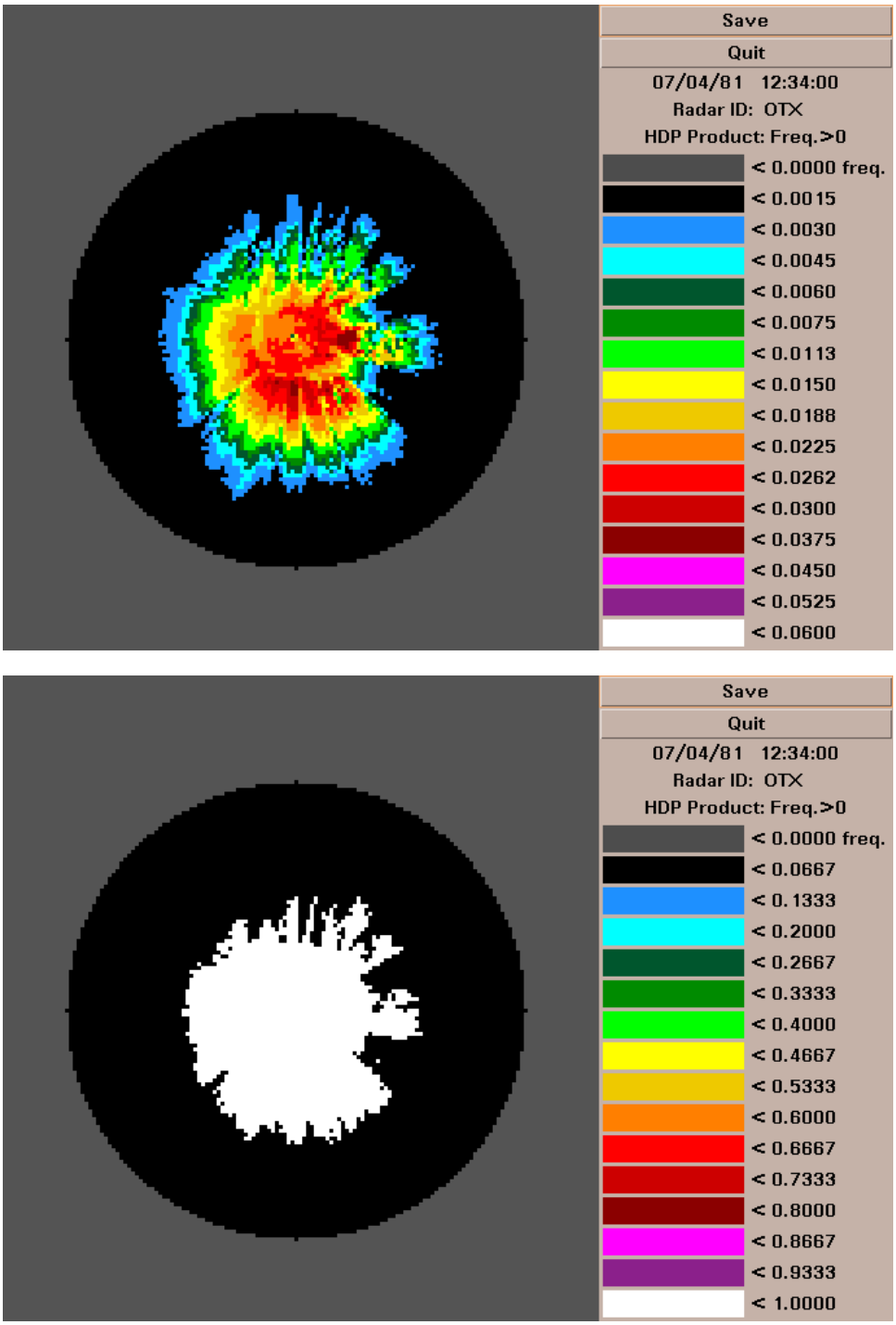

Figure 16. Spokane, WA cool season climatology a) Frequency of Rainfall b) Radar coverage map (white = good coverage)

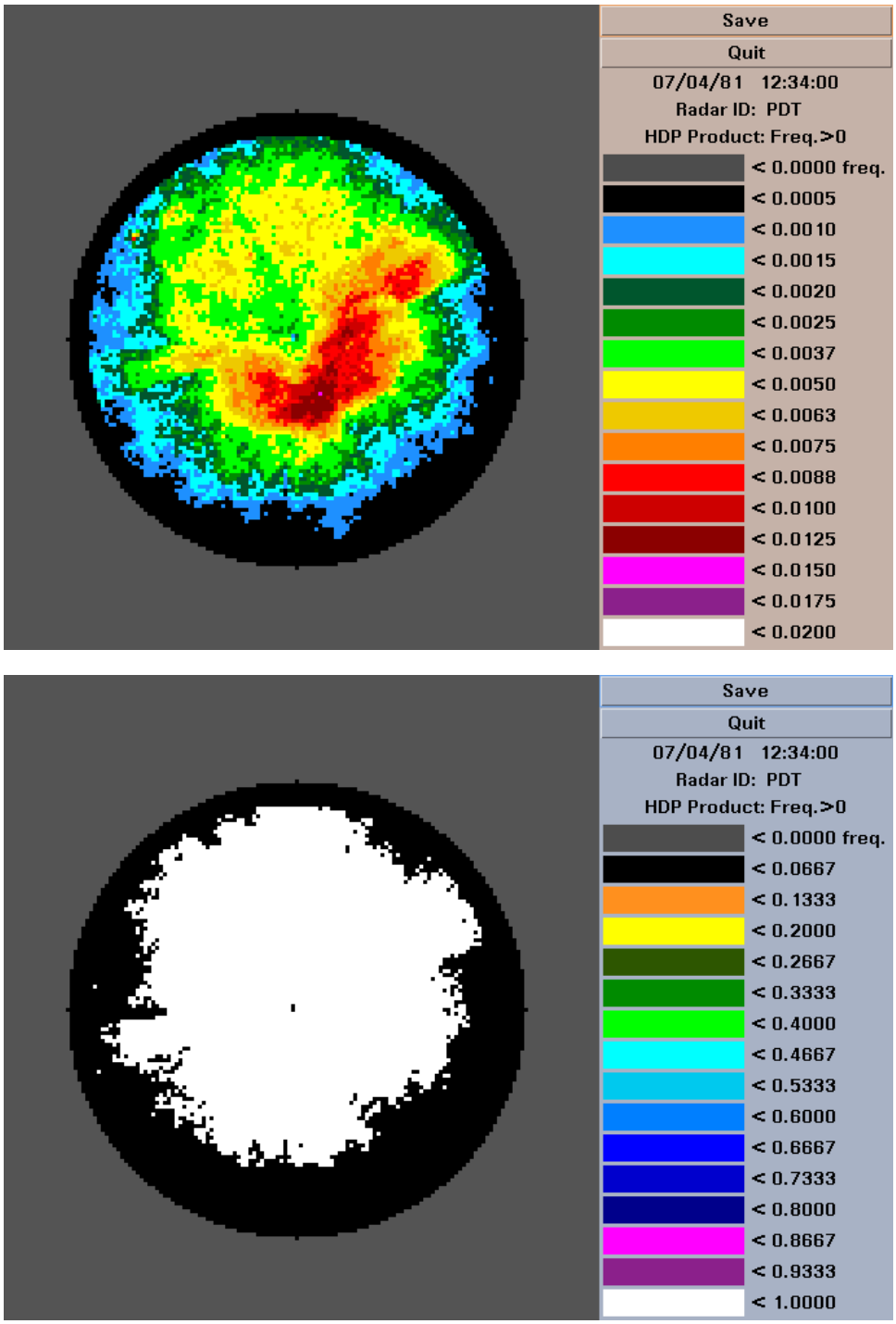

Figure 17. Pendleton, OR, warm season climatology a) Frequency of Rainfall b) Radar coverage map (white = good coverage)

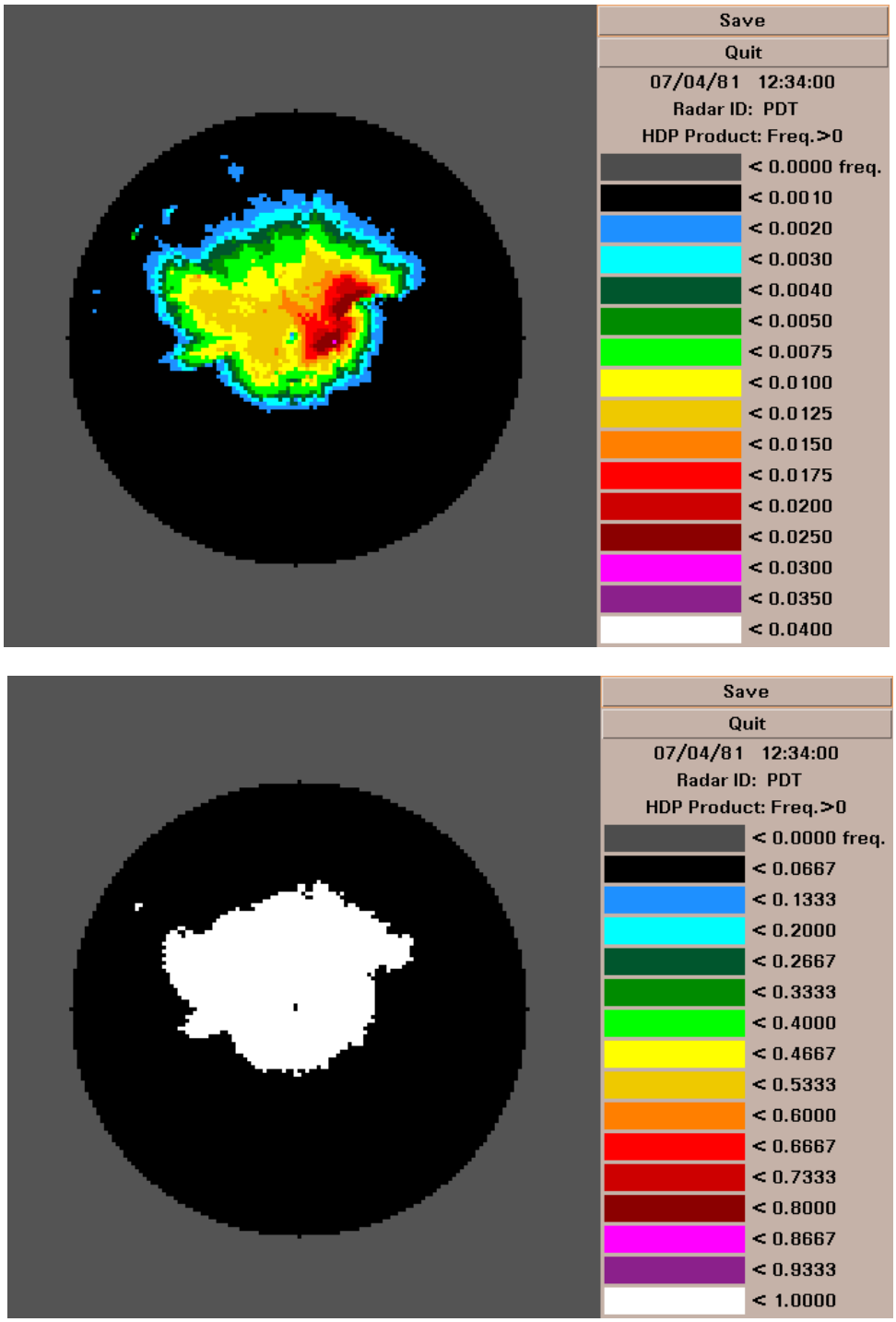

Figure 18. Pendleton, OR cool season climatology a) Frequency of Rainfall b) Radar coverage map (white = good coverage)

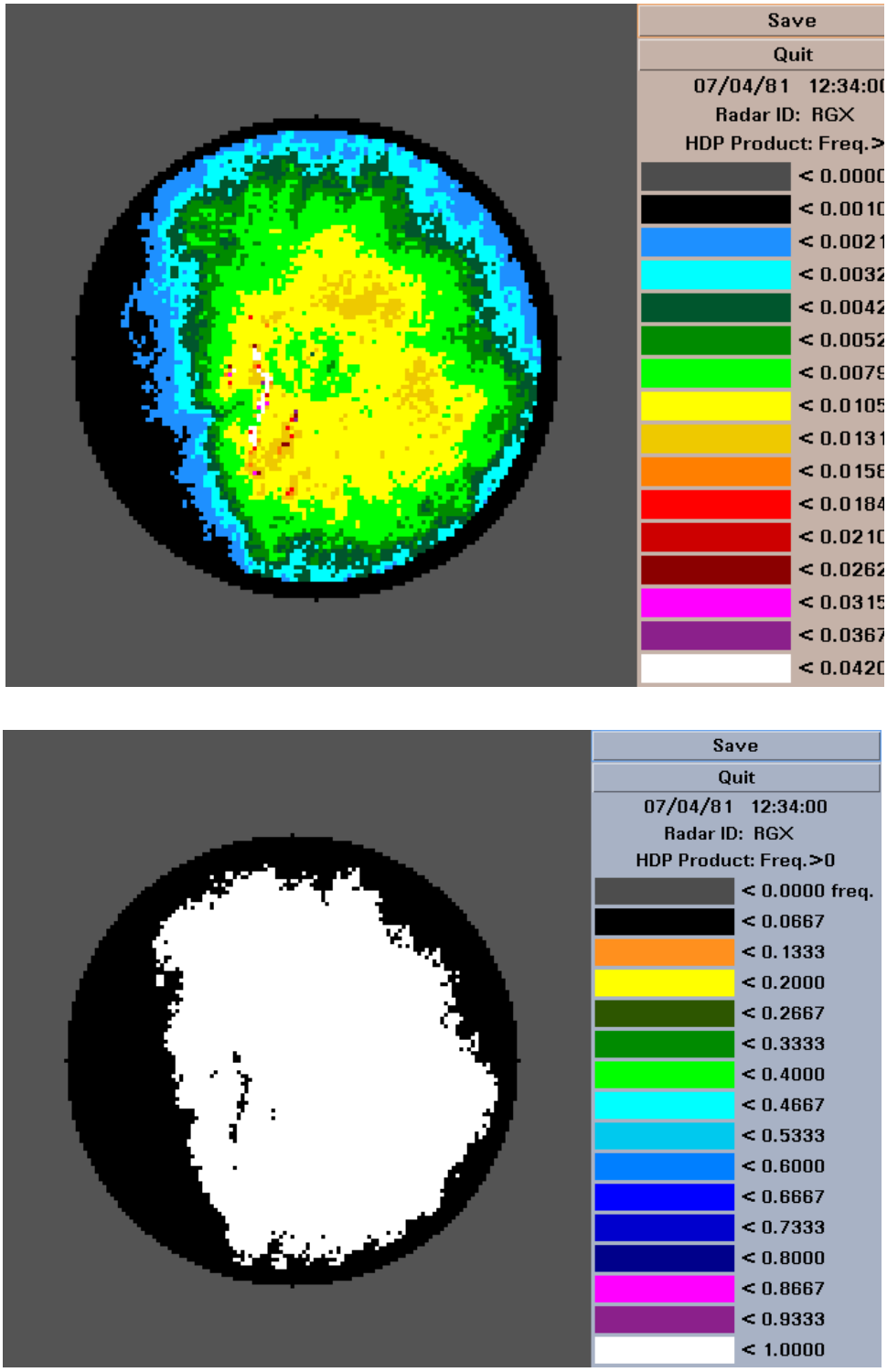

Figure 19. Reno, NV warm season climatology a) Frequency of Rainfall b) Radar coverage map (white = good coverage)

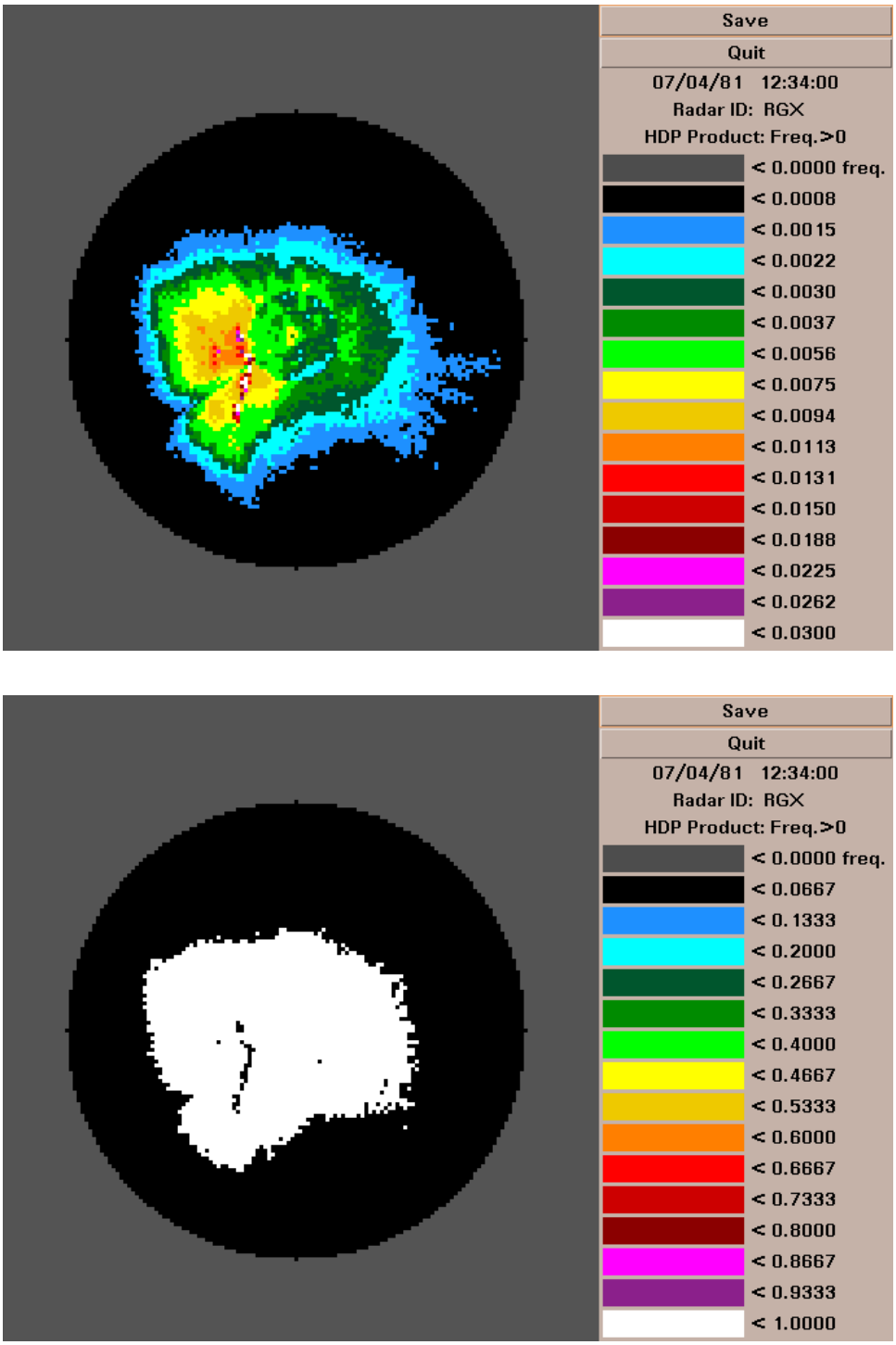

Figure 20. Reno, NV cool season climatology a) Frequency of Rainfall b) Radar coverage map (white = good coverage)

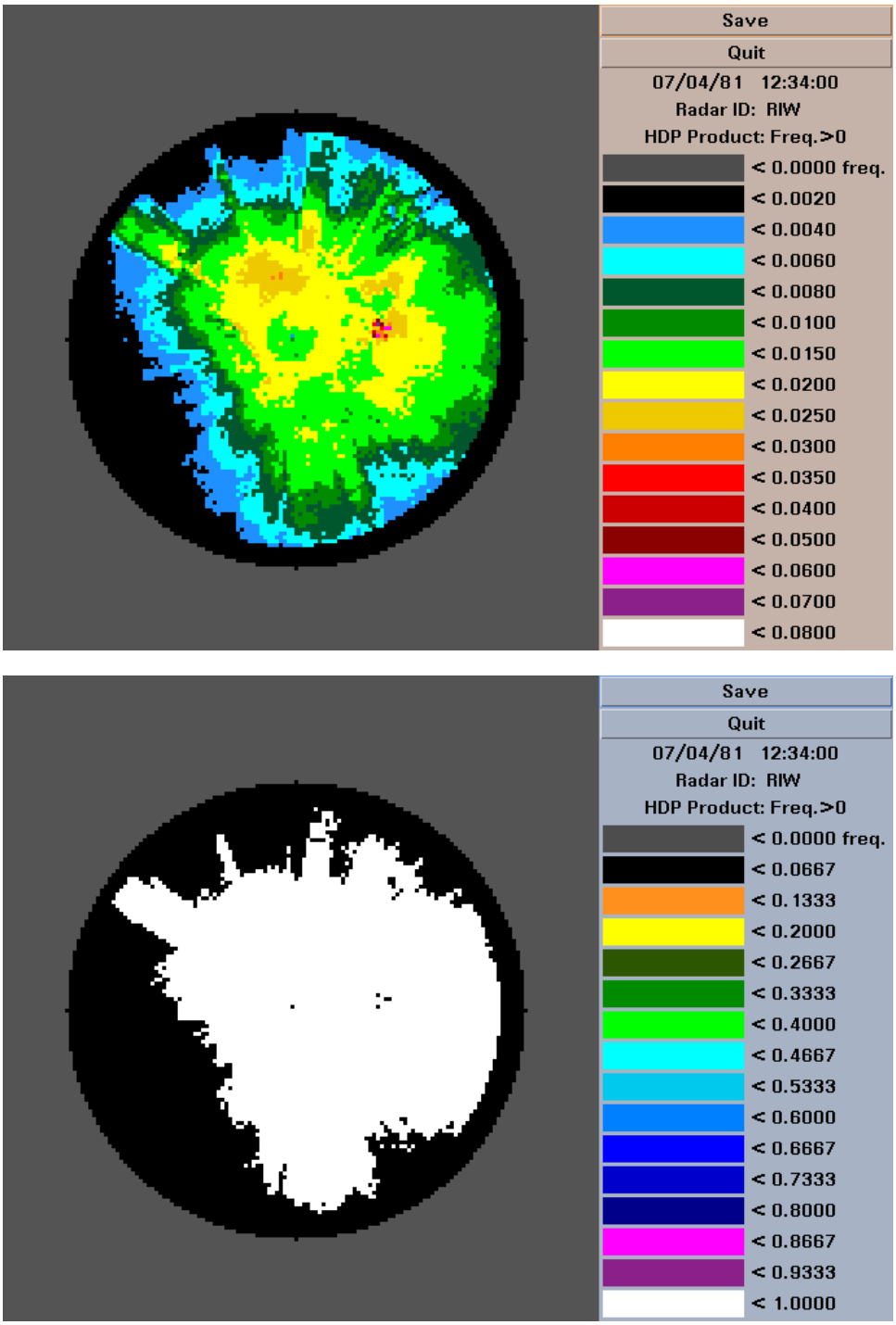

Figure 21. Riverton, WY warm season climatology a) Frequency of Rainfall b) Radar coverage map (white = good coverage)

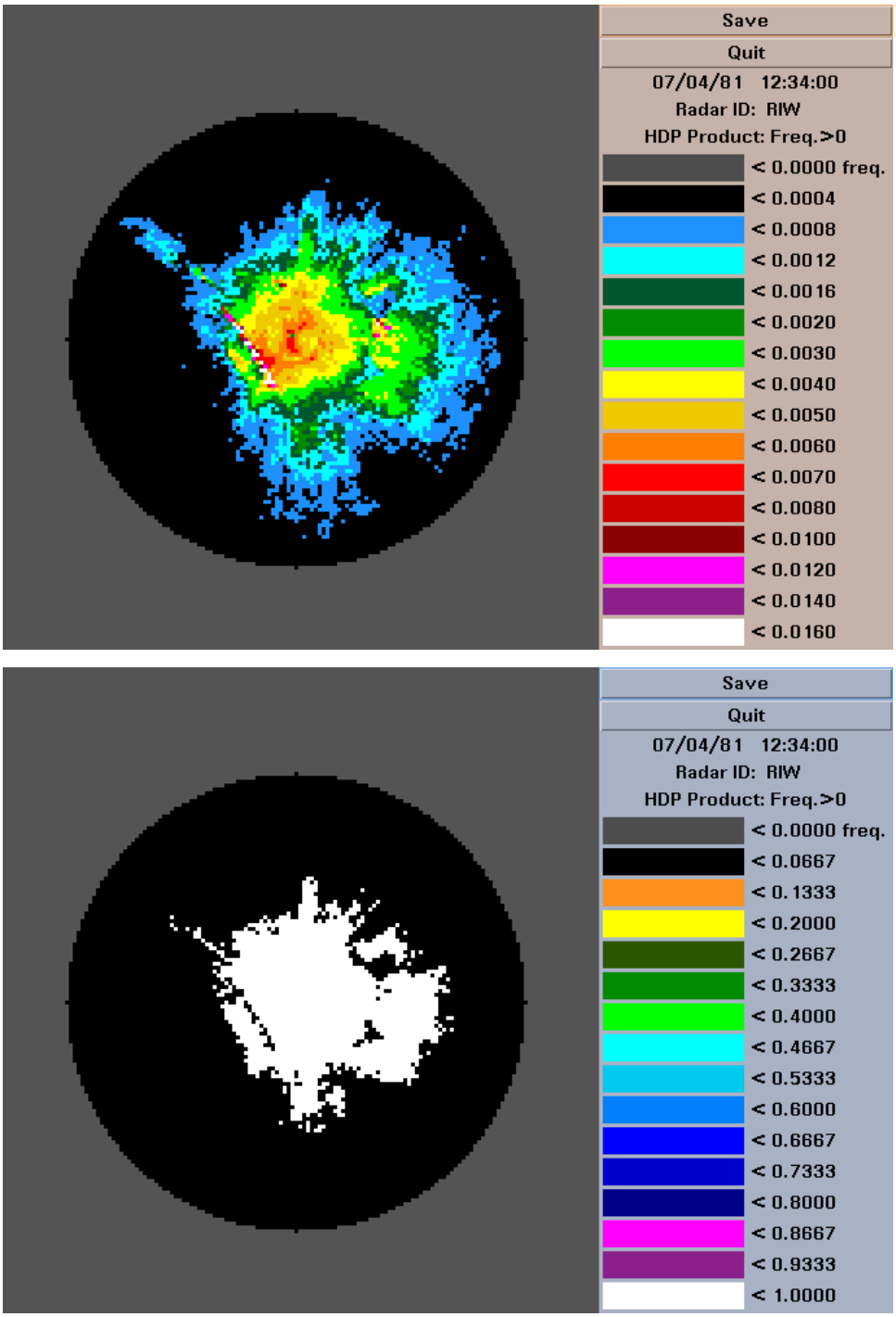

Figure 22. Riverton, WY cool season climatology a) Frequency of Rainfall b) Radar coverage map (white = good coverage)

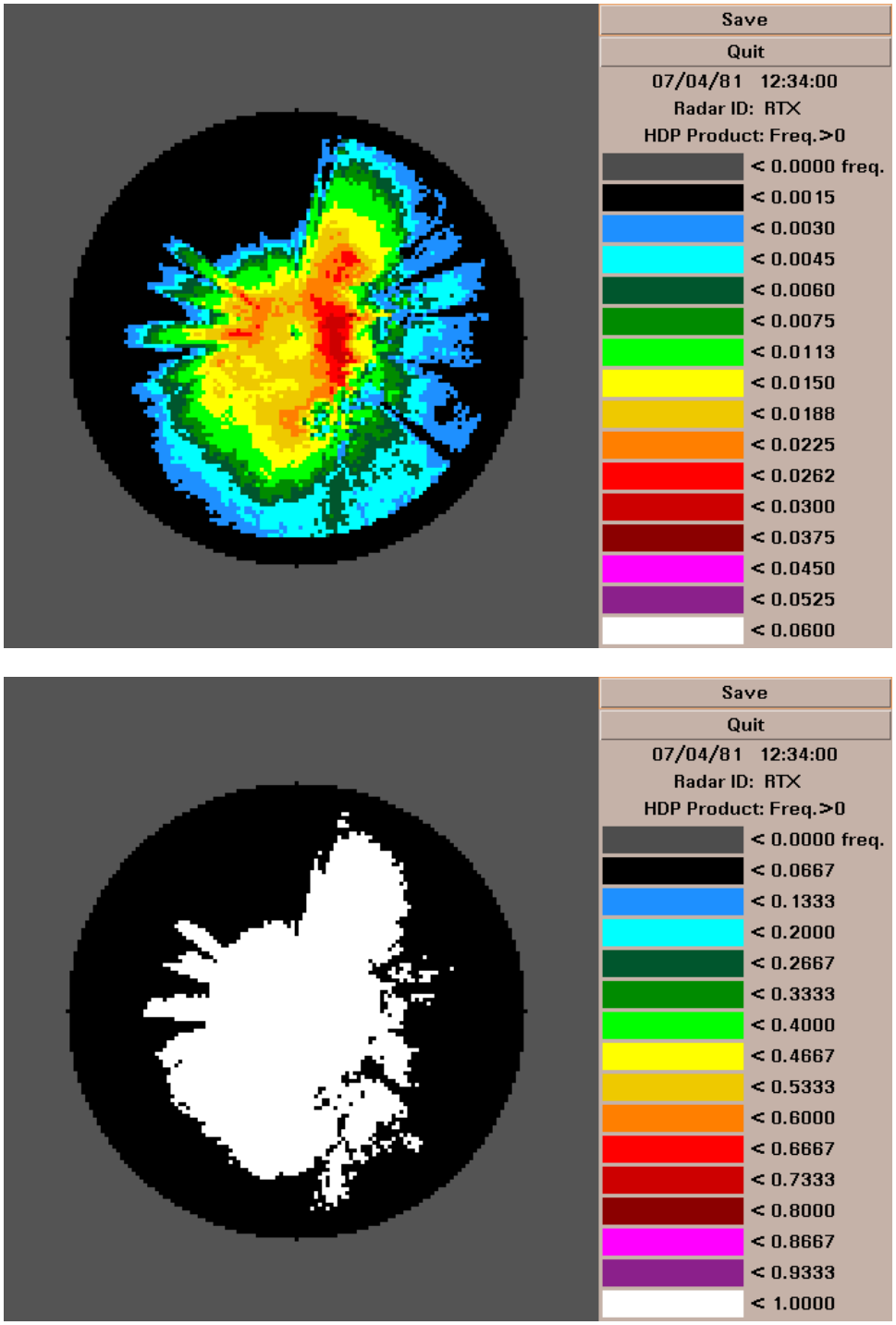

Figure 23. Portland, OR warm season climatology a) Frequency of Rainfall b) Radar coverage map (white = good coverage)

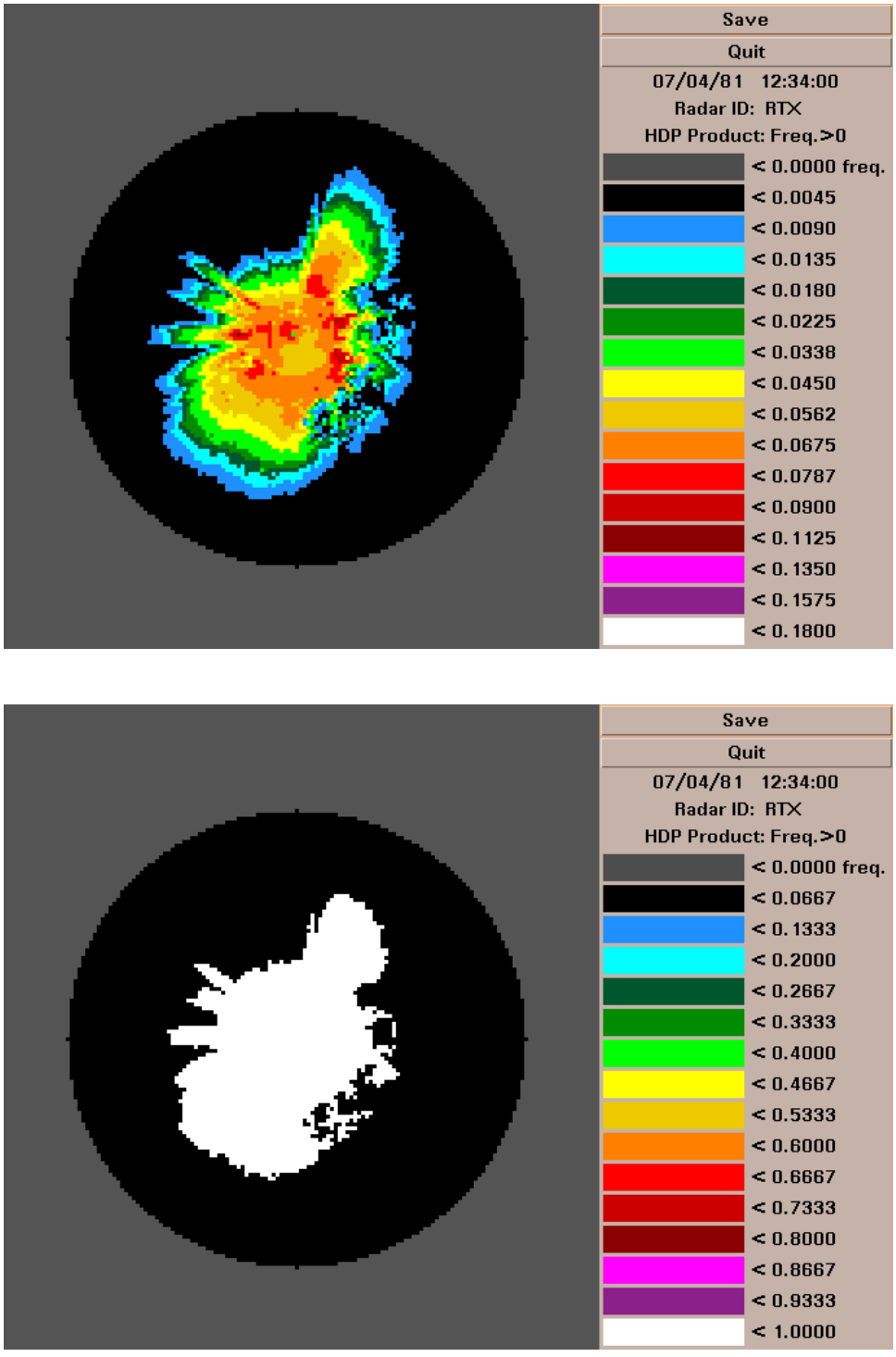

Figure 24. Portland, OR cool season climatology a) Frequency of Rainfall b) Radar coverage map (white = good coverage)

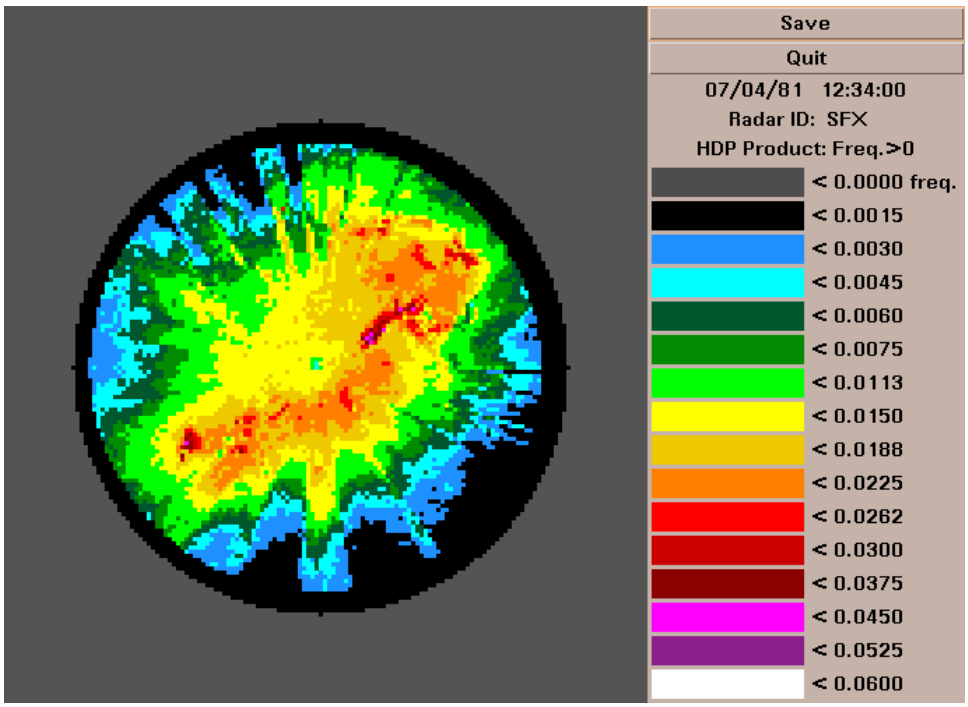

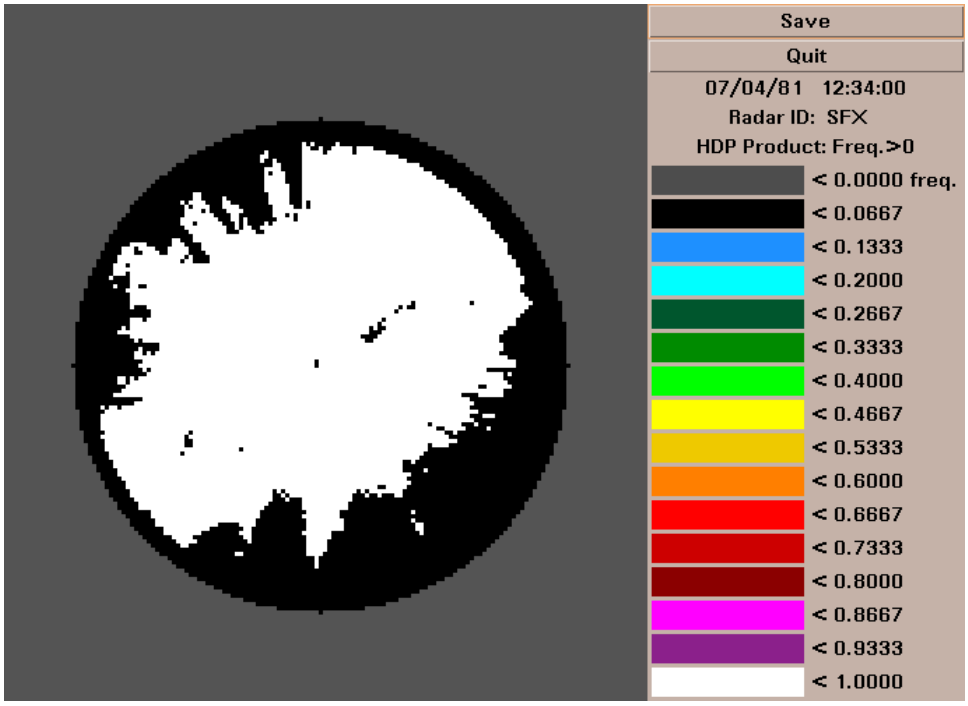

Figure 25. Pocatello, ID warm season climatology a) Frequency of Rainfall b) Radar coverage map (white = good coverage)

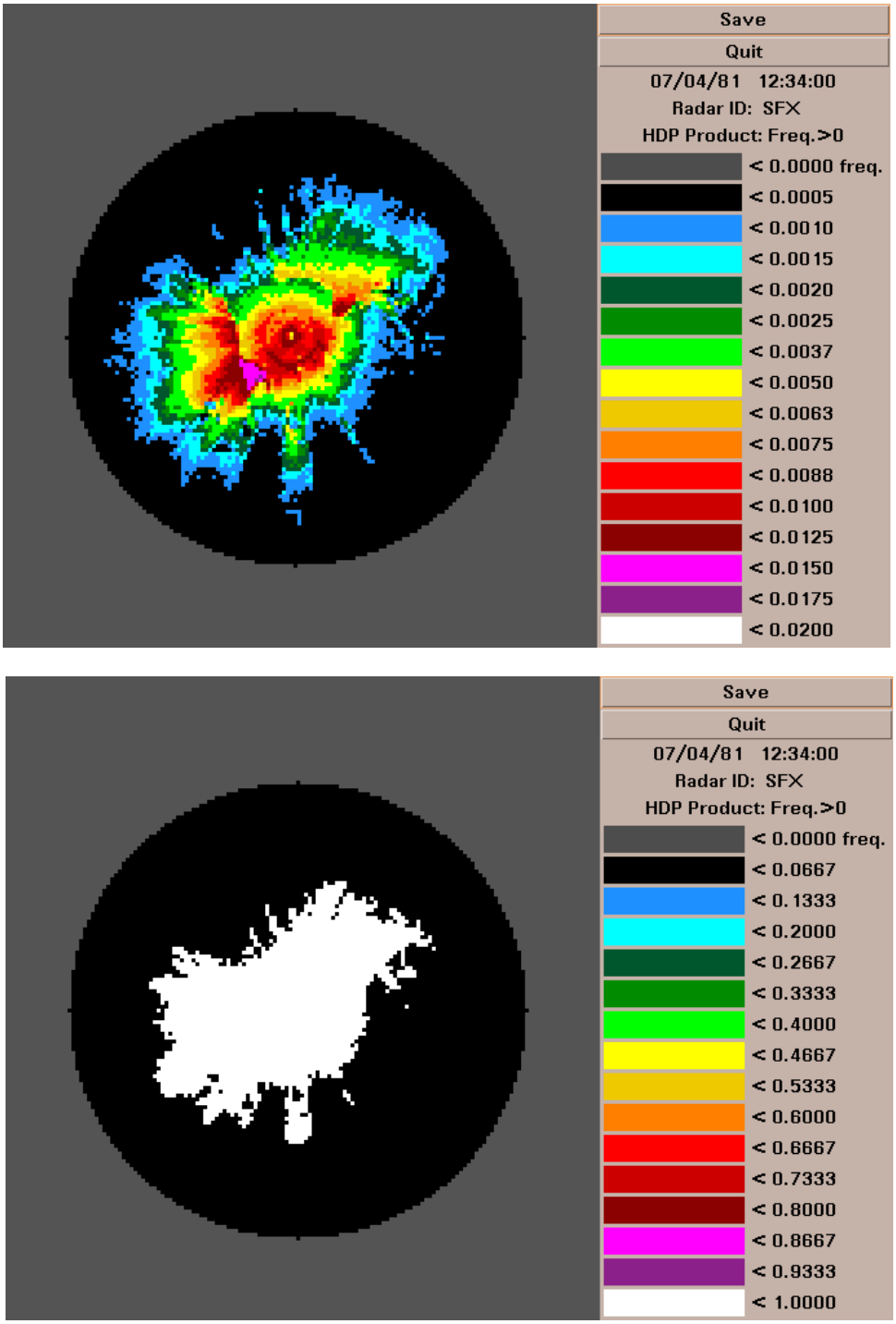

Figure 26. Pocatello, ID cool season climatology a) Frequency of Rainfall b) Radar coverage map (white = good coverage)

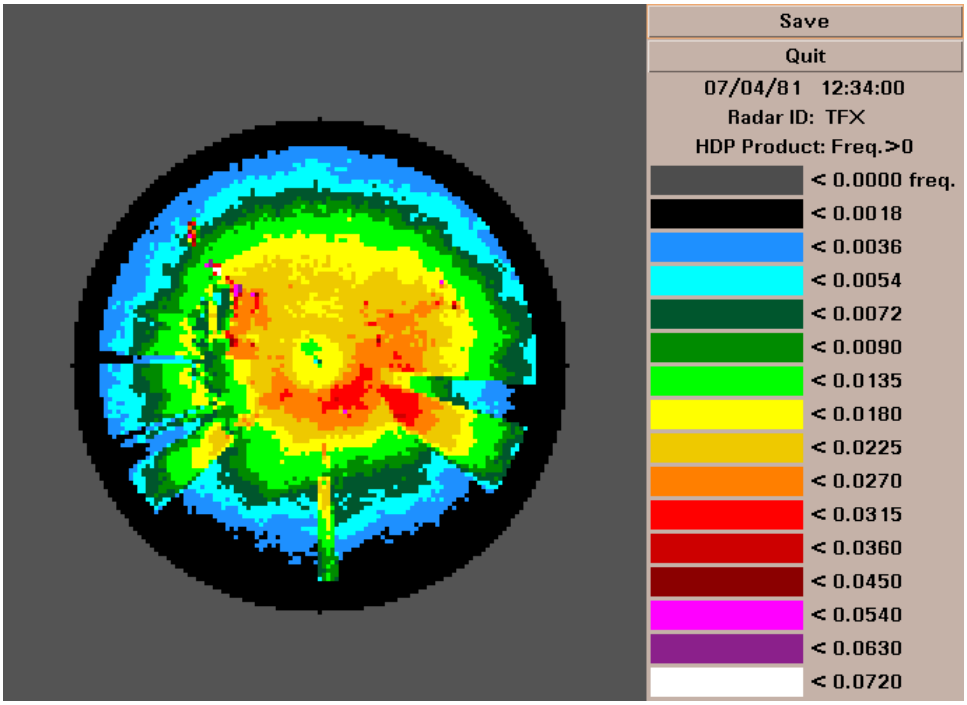

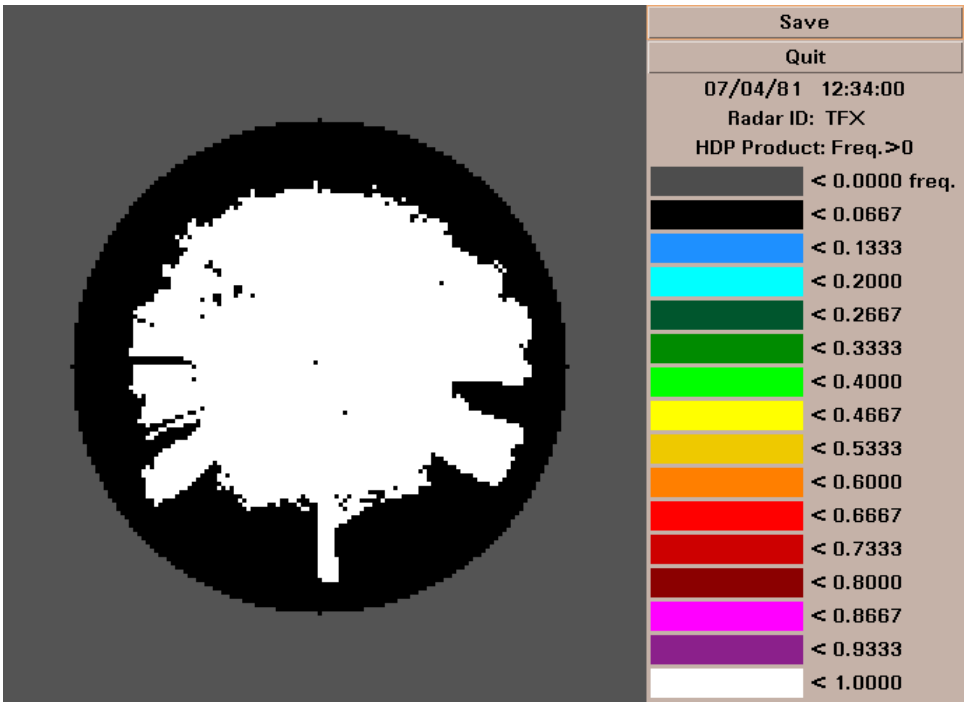

Figure 27. Great Falls, MT warm season climatology a) Frequency of Rainfall b) Radar coverage map (white = good coverage)

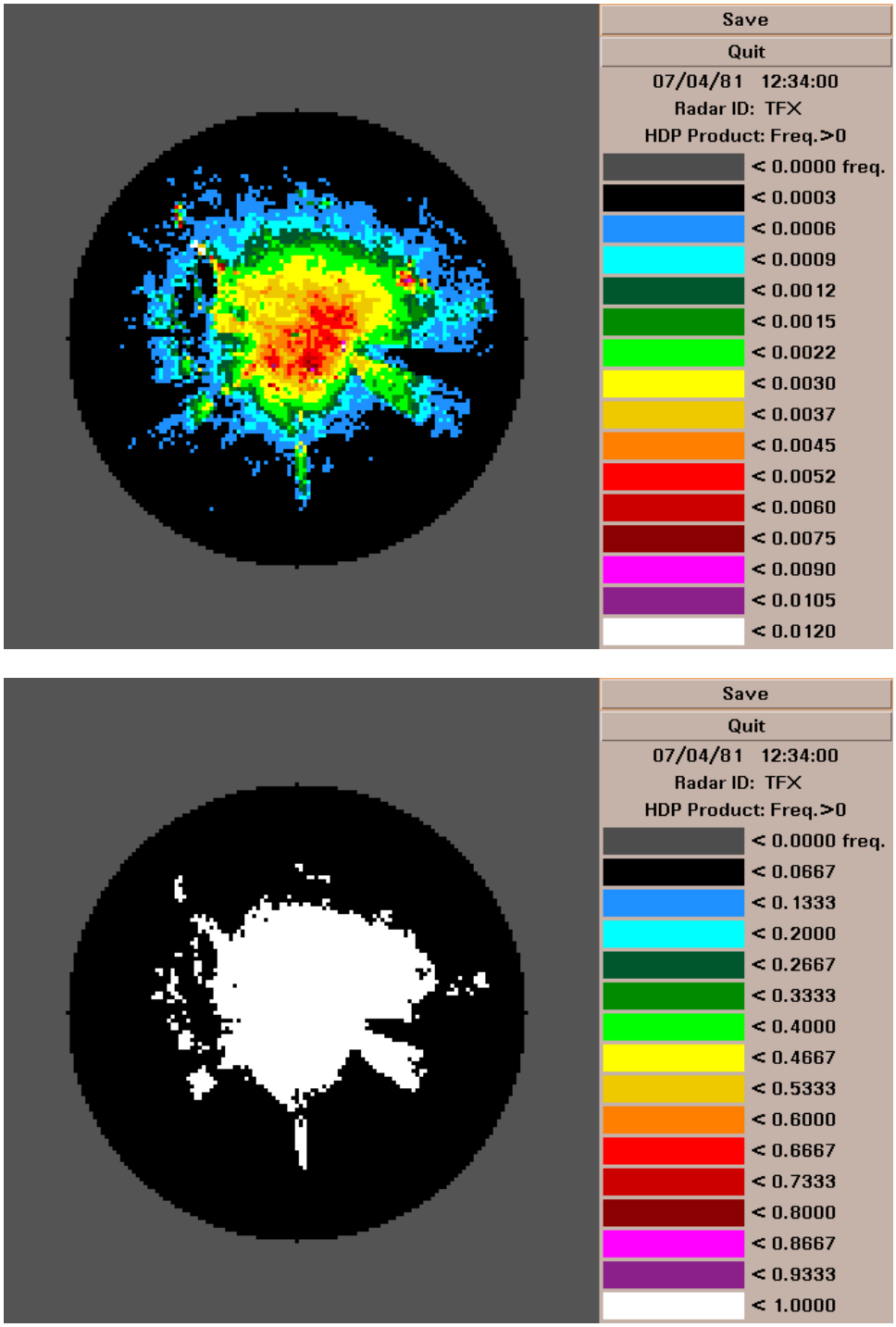

Figure 28. Great Falls, MT cool season climatology a) Frequency of Rainfall b) Radar coverage map (white = good coverage)

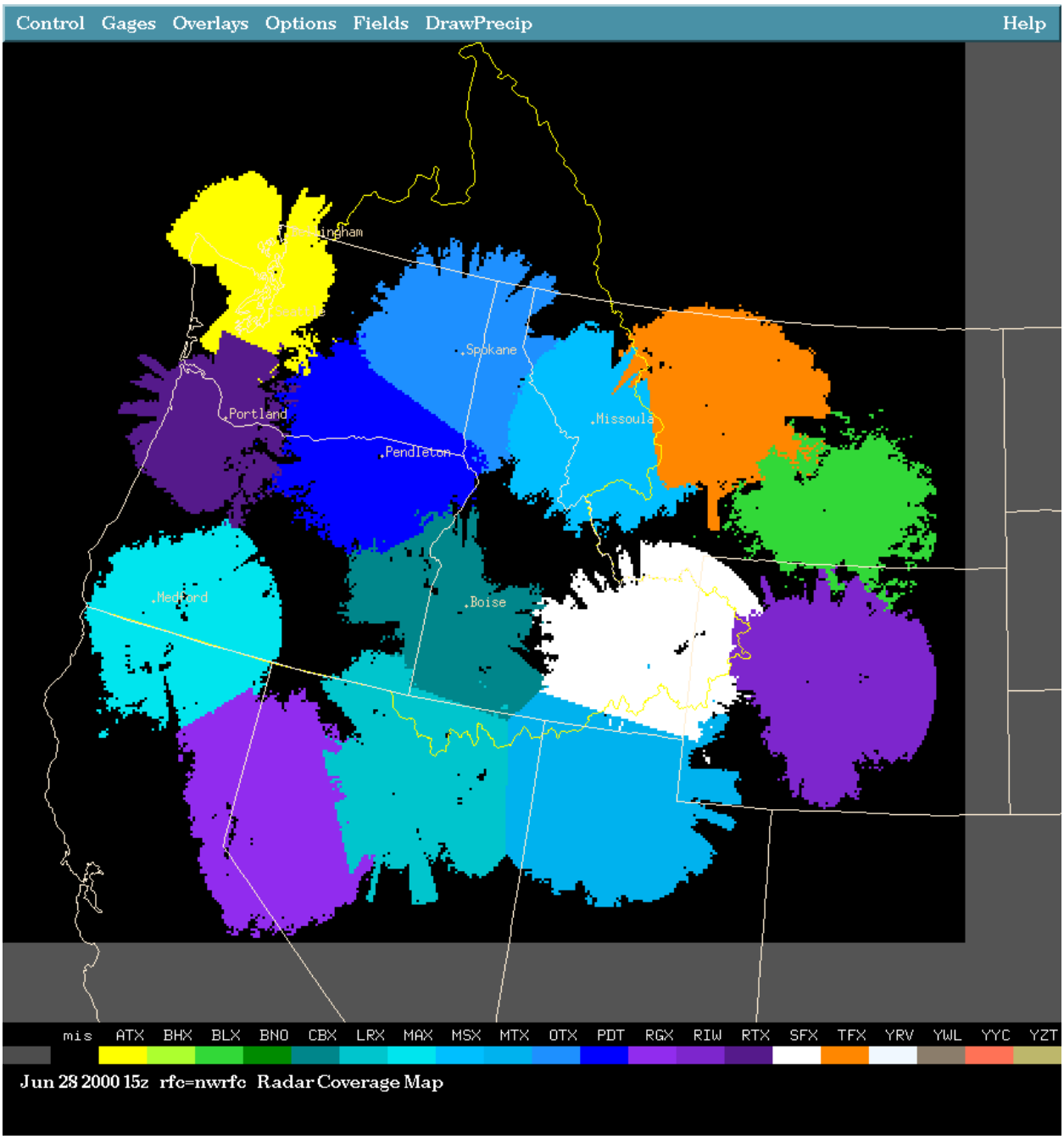

Figure 29. Warm season multi-radar coverage map for NWRFC using lowest available radar coverage for mosaic. RFC-boundary indicated with yellow line.

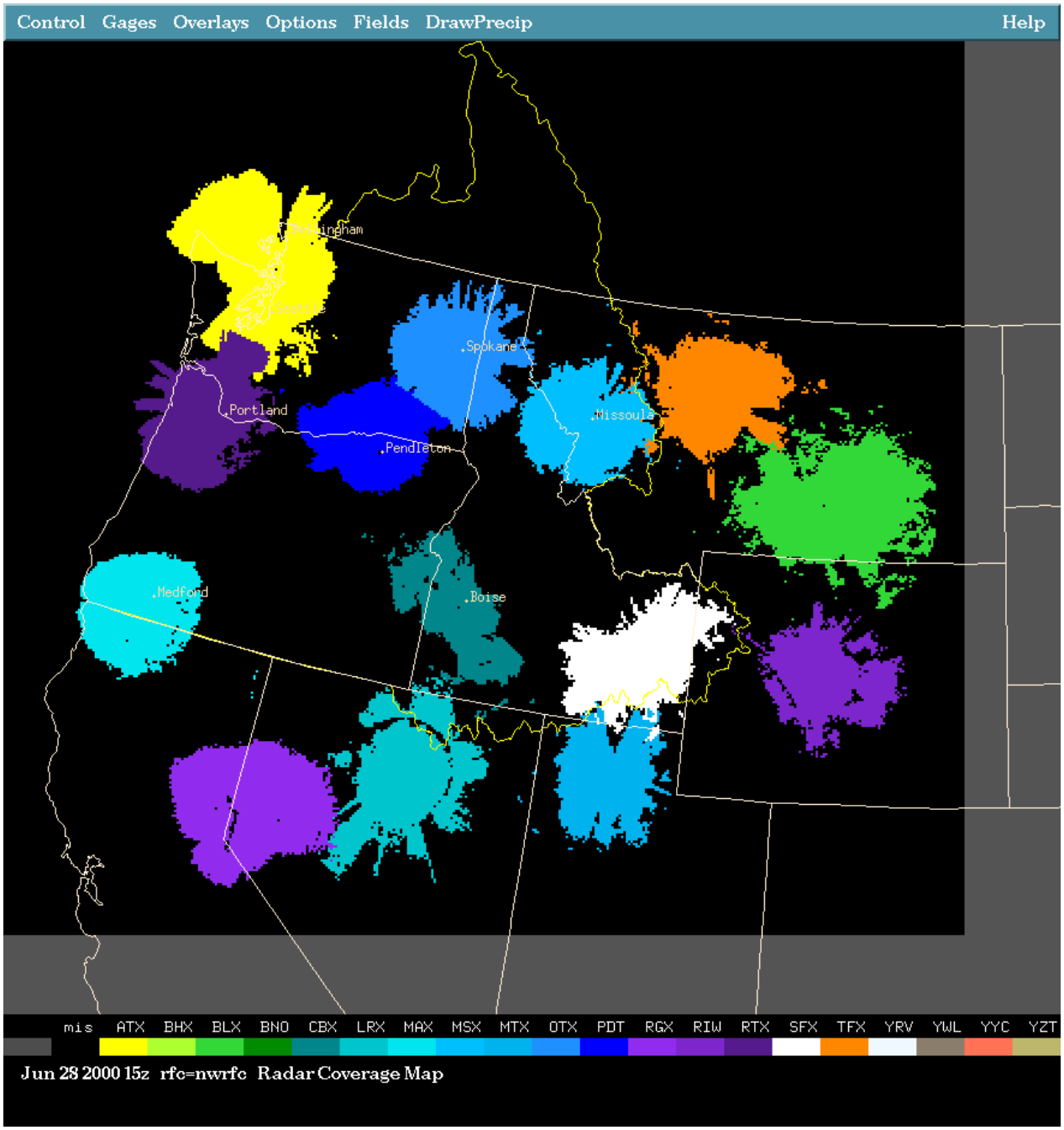

Figure 30. Cool season multi-radar coverage map for NWRFC using lowest available radar coverage for mosaic. RFC-boundary indicated with yellow line.

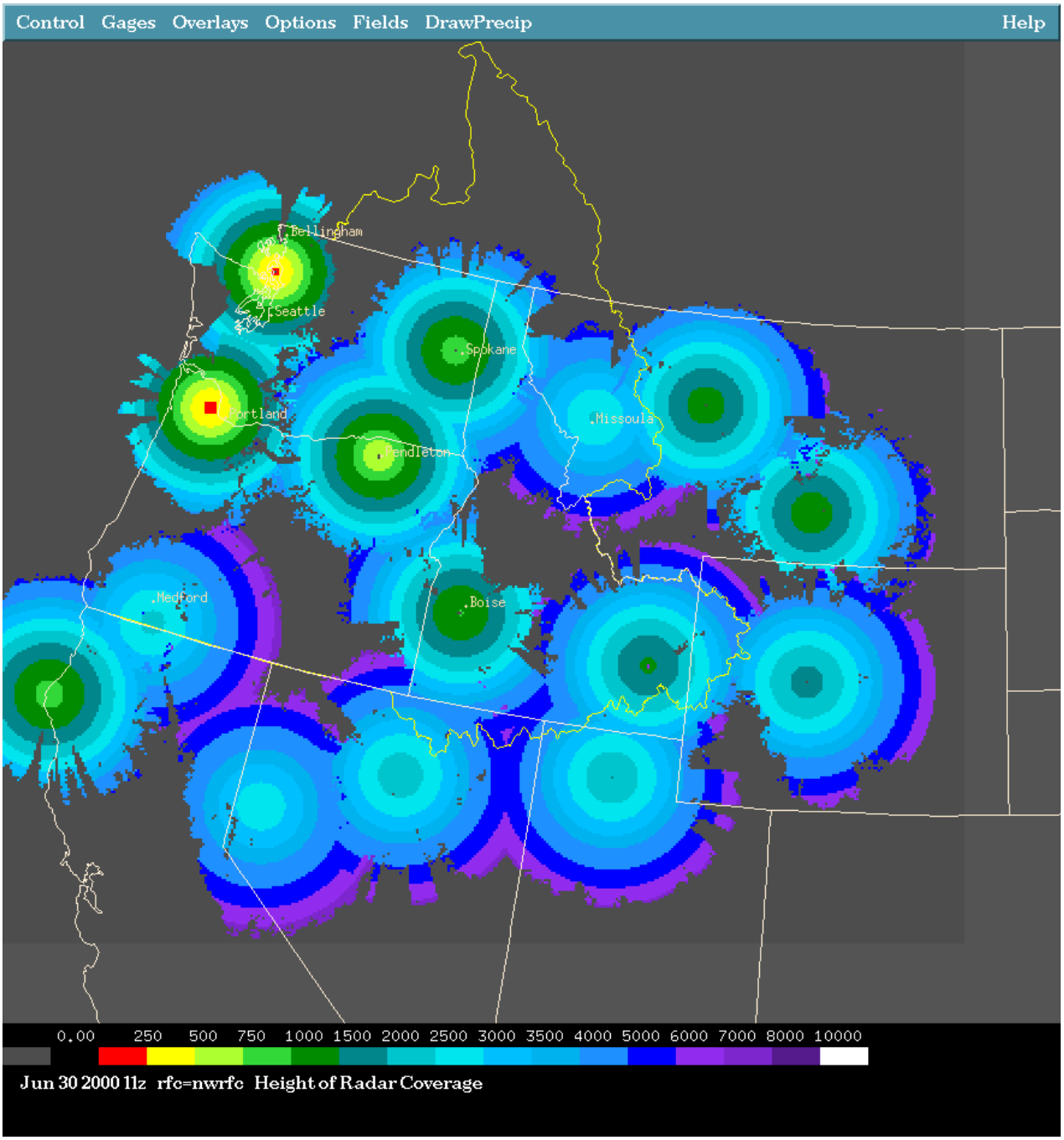

Figure 31. Height of lowest available radar coverage in warm season for NWRFC in meters above sea level.

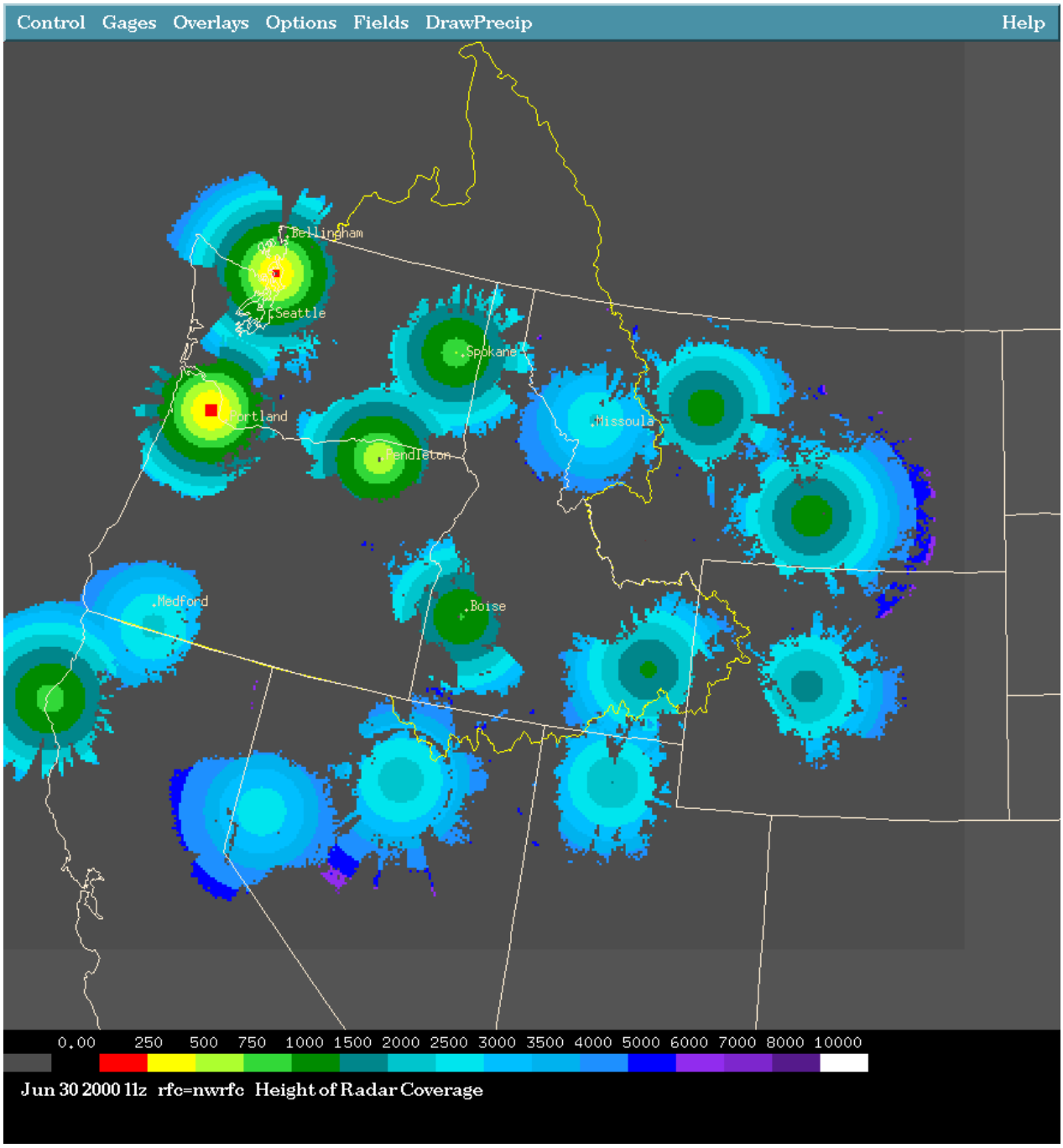

Figure 32. Height of lowest available radar coverage in cool season for NWRFC in meters above sea level.

4. References

Fulton, R.,J. Breidenbach, D.J. Seo, D.Miller, and T. O'Bannon, 1998: The WSR-88D Rainfall Algorithm. Weather and Forecasting,**13**, 377-395.

O'Bannon, T., 1997: Using a "Terrain-based" Hybrid Scan to improve WSR-88D precipitation estimates. Preprints, 28th Conf. On Radar Meteor., Austin TX, Amer. Meteor. Soc., 506-507.

Klazura, G. E., J. M. Thomale, D. S Kelly, P. Jendrowski, 1999: A Comparison of NEXRAD WSR-88D Radar Estimates of Rain Accumulation with Gauge Measurements for High- and Low- Reflectivity Horizontal Gradient Precipitation Events, Journal of Atmospheric and Oceanic Tech., 16, 1842-1850.

Smith, J. A., M.L. Baeck, M. Steiner, B. Bauer-Messmer, W. Zhao, A. Tapia, 1996: Final Report, Hydrological Assessments of the NEXRAD Rainfall Algorithms. Submitted as part of the Interagency Memorandum of Understanding among the NEXRAD Program, WSR-88D Operational Support Facility, and the NWS/OH Hydrologic Research Laboratory. [Available from NWS/OH/HRL, 1325 East-West Hwy., W/OH1 Silver Spring, MD 20910]